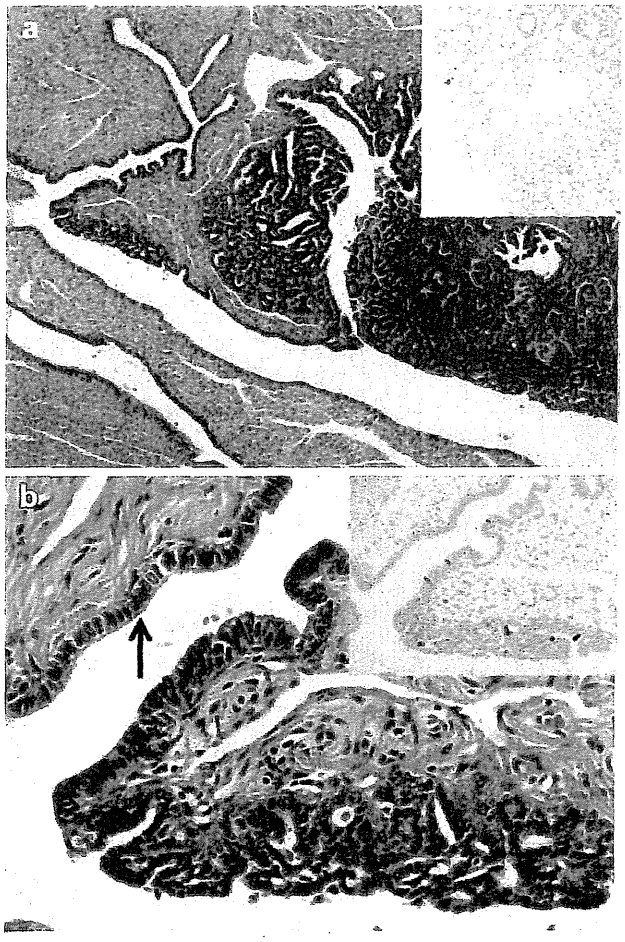

Fig. 2 Mucosal carcinoma of the fallopian tube detected in case 1. **a** Low-power view of the tubal low-grade serous adenocarcinoma. Predominant component of the tumor was noninvasive (in situ). However, some foci of microinvasion were observed. Tubal carcinoma was negative for p53 (*inset*). **b** High-power view of the tubal low-grade serous carcinoma and benign background tubal mucosa (*arrow*). Tumor cells with only mild atypia grew in complexed glandular structures and papillary structures. Immunostaining for Ki-67 is shown in the *inset*. Although the tubal carcinoma showed higher MIB-1 index in comparison with the benign tubal epithelium, its MIB-1 index was no more than 5%

between mucosal carcinomas of the fallopian tube and ovarian carcinomas in general populations to date [8, 10, 11, 15]. In these reports, the authors focused primarily on high-grade serous carcinogenesis and p53 alterations involved in the process. Other histological subtypes of ovarian cancer have not been studied in detail for coexisting tubal lesions. In fact, none of the past series included ovarian clear cell adenocarcinomas, which sometimes resemble serous adenocarcinoma histologically and pose difficult problems to surgical pathologists. In this study, we examined Japanese ovarian and peritoneal cancer cases, which included a large number of ovarian non-serous adenocarcinomas. The high prevalence of clear cell adenocarcinomas in our series should be attributed to the Japanese patient background. By comparing four major histological subtypes of ovarian carcinoma (serous, clear cell, endometrioid, and mucinous), we demonstrated that the coexistence of mucosal carcinoma of the fallopian tube was specific to cases of serous adenocarcinoma. The results of our study suggest that tubal lesion is unlikely to be associated with the development of ovarian clear cell adenocarcinomas and other non-serous adenocarcinomas. Thus, with regard to the origin of non-serous ovarian cancer, attention should rather be paid to the ovarian surface epithelium, inclusion cysts, and endometriotic lesions.

In our study, coexisting mucosal carcinoma of the fallopian tube was found in seven of 15 serous adenocarcinoma cases. The incidence of coexisting mucosal carcinoma and frequency of fimbrial involvement were similar to the values reported previously [8, 10, 15]. However, the p53 immunophenotype of mucosal carcinomas of the fallopian tube in our series was different from those in previous reports. In contrast to the previous series, which showed that nearly all mucosal carcinomas of the fallopian tube were immunohistochemically p53-positive [8, 10], more than half of the tubal lesions in our series were p53-negative. In this report, we hope to emphasize the existence of p53-negative mucosal carcinomas of the fallopian tube. Considering that more than 30% of high-grade serous adenocarcinomas are p53-negative immunohistochemically [26], it is reasonable that we encounter occasional p53-negative early tubal carcinomas that coexist with p53-negative high-grade ovarian/peritoneal serous adenocarcinomas. In general, a cautious approach is necessary in the evaluation of p53 immunoreactivity, especially when assessing the involvement of *TP53* mutations. It is well known that diffuse nuclear p53 immunoreactivity suggests the presence of such mutations. Importantly, studies have revealed that protein-truncating *TP53* mutations can lead to completely negative immunoreactivity [27]. On the other hand, a few scattered p53-positive cells by immunohistochemistry suggest that the lesion harbors wild-type *TP53*. In our series, most of the high-grade serous adenocarcinoma cases, including their coexisting tubal lesions, scored either as P (positive) or CN (completely negative) in immunoreactivity for p53. Therefore, it is highly likely that these tumors harbor *TP53* mutations, and we believe *TP53* alterations play a significant role in the tumorigenesis of many tubal mucosal carcinomas.

Another striking finding in our study was the presence of tubal mucosal carcinoma coexisting with ovarian low-grade serous adenocarcinoma. Currently, not much is known about tubal low-grade serous adenocarcinoma, and there has been no report on the coexistence of tubal mucosal carcinoma in an ovarian low-grade serous adenocarcinoma

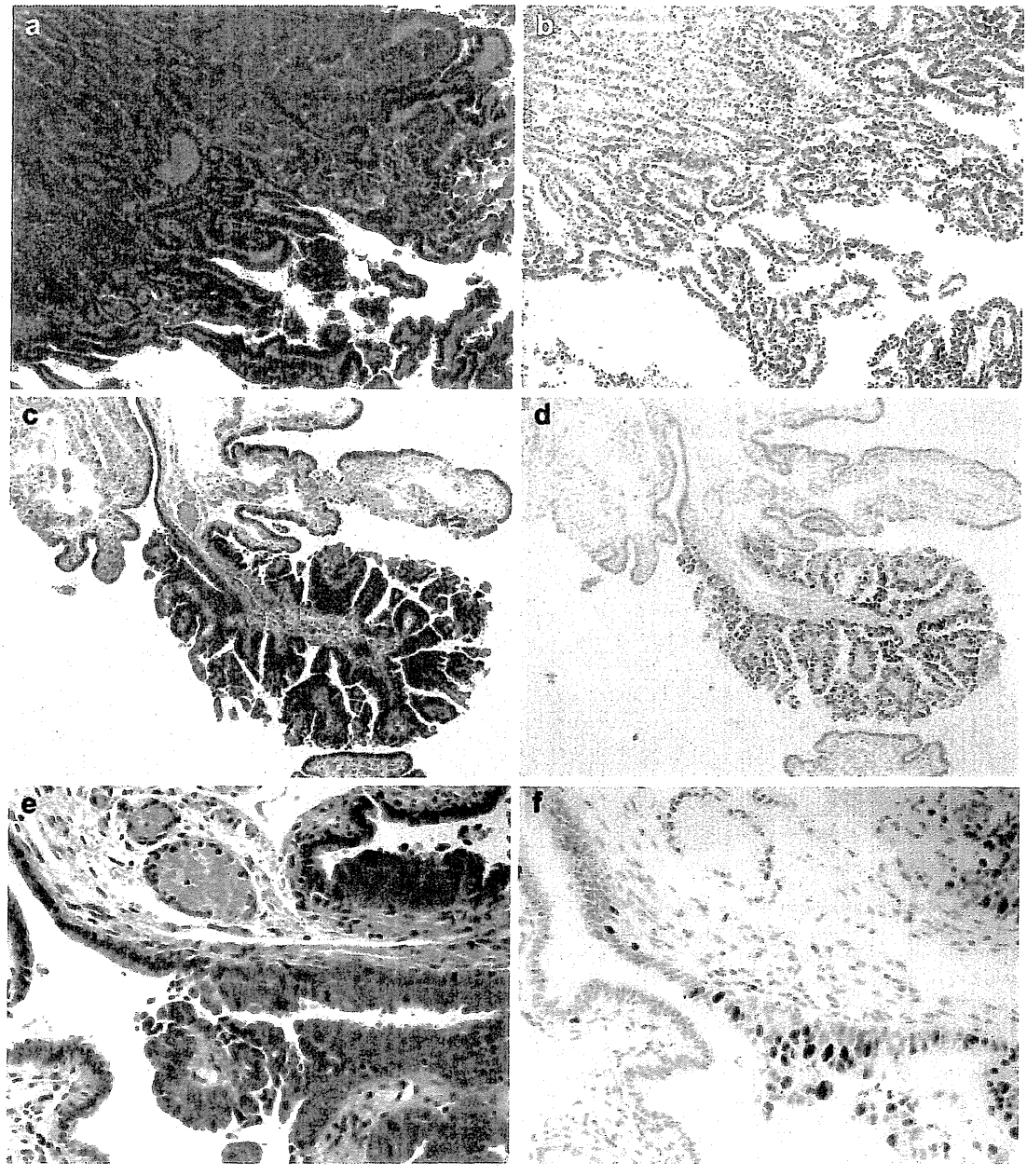

Fig. 3 Histology of ovarian tumor and coexisting mucosal carcinoma of the fallopian tube in case 2. **a** Ovarian carcinoma was high-grade serous adenocarcinoma showing papillary pattern of growth. **b** Ovarian high-grade serous adenocarcinoma showing diffuse immunoreactivity for p53. **c** Mucosal carcinoma of the fallopian tube detected in the fimbriae. **d** Mucosal carcinoma of the fallopian tube was p53-positive. **e** High-power view of the mucosal carcinoma of the fallopian tube. Tumor cells with moderate to severe atypia showing intraepithelial growth. **f** MIB-1 index of the mucosal carcinoma of the fallopian tube was elevated markedly (>50%), compared to adjacent benign mucosa

case. In our case, the tubal lesion showed prominent papillary growth and was large enough to be readily recognized upon microscopic examination. However, cytological atypia of this low-grade tubal carcinoma was very mild, and only a slight increase in MIB-1 index was seen. In addition, p53 immunohistochemistry revealed a wild-type *TP53* phenotype. Based on our experience, we believe that such low-grade tubal lesions can be diagnosed only by means of thorough histological examination, as immunohistochemistry may not always be helpful. Initially, surgical pathologists should be made aware of the occurrence of tubal low-grade serous adenocarcinoma. Accumulation of information about low-grade tubal carcinomas will provide more insights into the pathogenesis of early tubal cancers,

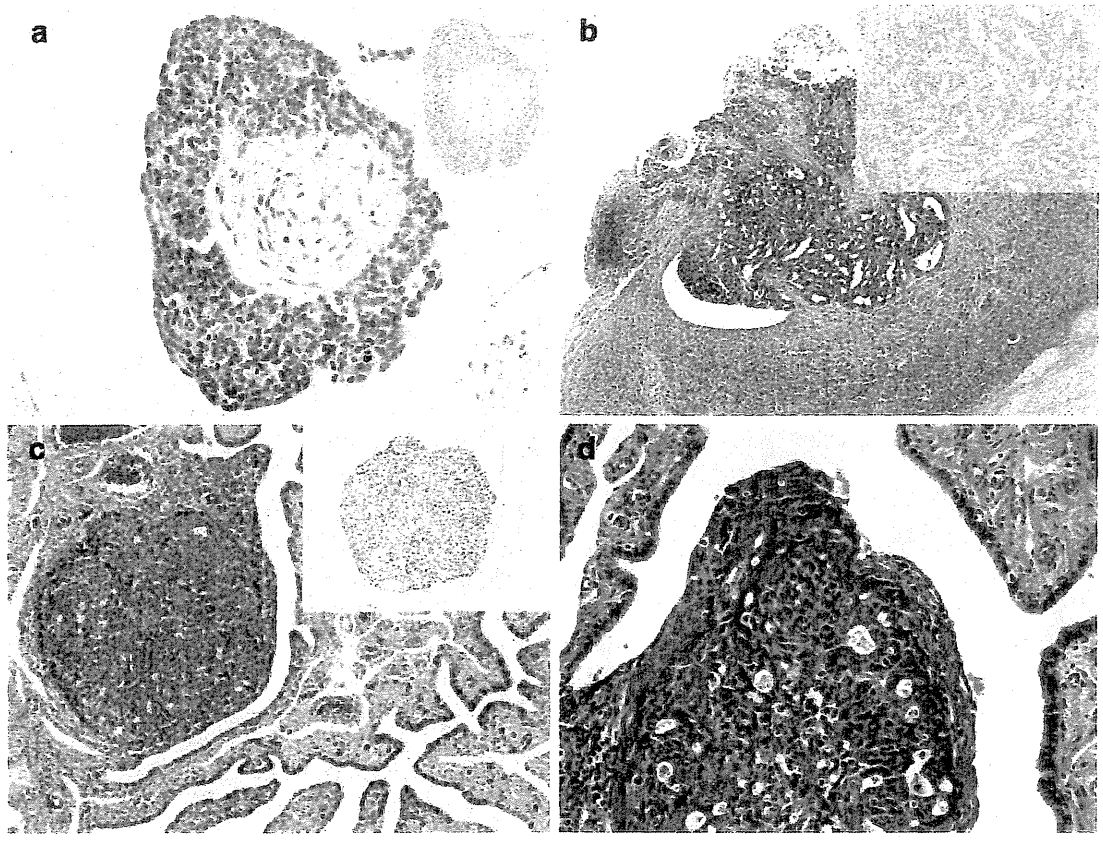

Fig. 4 Histological features of pelvic serous adenocarcinomas of case 14. **a** Nests of serous adenocarcinoma in the omentum, and p53 immunostaining (*inset*). Adenocarcinoma in the omentum is completely negative for p53. **b** Serous adenocarcinoma involving the ovarian surface and p53 immunostaining (*inset*). Adenocarcinoma in the ovary is also completely negative for p53. **c** A well-circumscribed nodule of serous adenocarcinoma detected in the submucosa of the left fallopian tube, and p53 staining (*inset*). The tubal lesion is diffusely positive for p53. **d** A deeper section of the left tubal carcinoma revealed tumor exposure in the tubal mucosa. However, no intraepithelial carcinoma was detected in the adjacent tubal mucosa

including their potential association with ovarian low-grade serous adenocarcinomas.

Regarding p53 alterations in the fallopian tube, we also evaluated the existence of p53 signatures in the background tubal mucosa. The p53 signature has been recognized as a lesion that will evolve to p53-positive mucosal carcinoma of the fallopian tube [14]. Studies have emphasized its importance as an initial change that occurs in pelvic serous carcinogenesis [11, 28]. Interestingly, the p53 signature has been reported to be equally prevalent in benign tubes of BRCA+ and control women [11]. In this series, the prevalence of p53 signatures was not significantly different between serous adenocarcinoma cases and clear cell adenocarcinoma cases. Based on this result, we assume that the presence of the p53 signature itself does not constitute a risk for developing p53-positive pelvic serous carcinoma. Rather, events that take place between the p53 signature and p53-positive mucosal carcinoma of the fallopian tube should be regarded as key steps in the carcinogenesis of p53-positive pelvic serous adenocarcinomas.

Theoretically, there are three ways of interpreting mucosal carcinoma of the fallopian tube: most importantly, as an "early carcinoma (preceding lesion) that progresses to form pelvic serous carcinoma," as a "disseminated serous carcinoma showing intraepithelial spread," or as a part of "multifocal (multiclonal) neoplastic lesions in the pelvis." Each theory has its strong points and weak points. Recent studies have provided evidence in support of the "preceding lesion" theory [7–11, 15]. The frequent presence of early tubal lesions in prophylactically removed specimens from BRCA carriers is an important rationale for designating mucosal carcinoma of the fallopian tube as a "preceding lesion," not just a "coexistent lesion." However, BRCA carriers comprise only about 10% of ovarian cancer patients [29–31], and incidence of mucosal carcinoma of the fallopian tube in patients without BRCA mutations remains unclear. In addition, the precise events that take place between the evolution of initial early tubal carcinoma and the development of mass-forming ovarian or peritoneal serous carcinoma have yet to be clarified. Thus, although

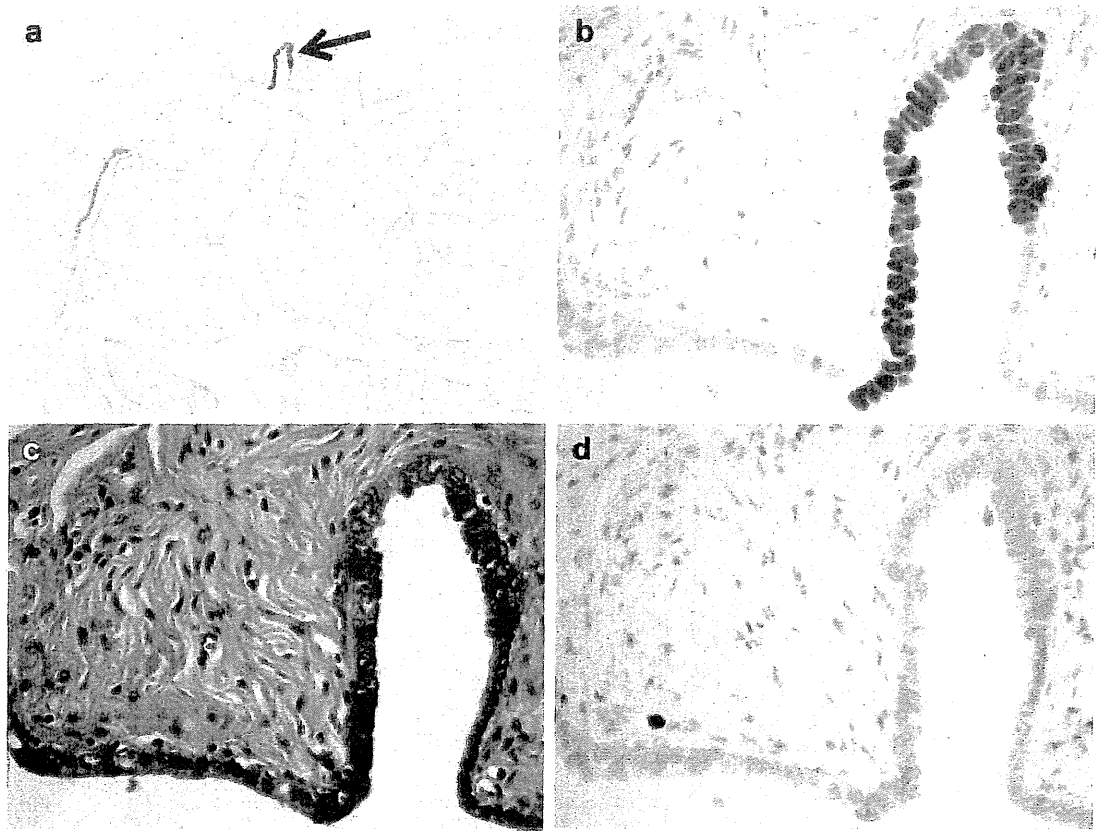

Fig. 5 p53 signatures in the background tubal epithelium of an ovarian clear cell adenocarcinoma case. **a** Immunostaining for p53. Multifocal p53 signatures were found in non-fimbriated tubal mucosa. **b** High-power view of a p53 signature (*arrow* in **a**), (**c**) its hematoxylin and eosin staining, and (**d**) its Ki-67 immunostaining. MIB-1 index of the p53 signature was 0%

we believe, based on the results of our study, that mucosal carcinoma of the fallopian tube is a candidate preceding lesion of pelvic serous adenocarcinoma, additional evidence is necessary to strengthen this hypothesis.

The possibility of some tubal mucosal carcinomas being cancer disseminations from remote tumors should also be discussed. In our series, seven of 13 serous adenocarcinomas with peritoneal disseminations had coexisting mucosal carcinomas of the fallopian tube. On the other hand, mucosal carcinoma of the fallopian tube was not identified in any of the eight non-serous adenocarcinomas with peritoneal disseminations. This result suggests that, in general, ovarian cancer dissemination rarely shows tubal intraepithelial spread. Consequently, it is rather unlikely that a significant number of mucosal carcinomas of the fallopian tube are disseminated carcinoma showing intraepithelial spread. However, in some of our cases, we experienced certain difficulties in making a strict histological distinction between primary intraepithelial neoplasm of the fallopian tube and cancer implantation involving the tubal mucosa. The distinction was especially problematic when the lesions were accompanied by inflammatory stroma and adjacent invasive carcinoma. Ancillary tests, such as immunohistochemistry and genetic studies, are not helpful in making such a distinction.

Finally, mucosal carcinoma of the fallopian tube might be viewed as a part of multifocal (multiclonal) pelvic tumors. Although previous molecular studies on mucosal carcinomas of the fallopian tube have indicated monoclonal origin of the tubal and ovarian tumors in most cases [8, 10, 11], the numbers of cases studied were small, and there were some exceptions. In a series by Salvador et al. [8], fluorescence in situ hybridization (FISH) analysis revealed the possible multiclonal origin of carcinomas involving the ovary and the fallopian tube in one of the cases. In another series, by Kindelberger et al. [10], a case of ovarian serous adenocarcinoma accompanied by two multiclonal tubal carcinomas was included. We have also seen a case of bilateral early tubal carcinomas with an intraepithelial component in the past, which suggested multifocal carcinogenesis in the fallopian tubes [32]. In addition, there has been a report on multiclonal origin for some peritoneal serous carcinomas in patients with BRCA1 mutation [30]. In the present study, the possibility of multiclonal serous

carcinogenesis was seriously considered in case 14, in which we evaluated numerous serous adenocarcinoma foci in the pelvis and found only one minute nodule in the left tube that was p53-positive. We did not identify a definite TIC component adjacent to the left tubal lesion. However, it is likely that the left tubal lesion is a primary p53-positive tubal serous adenocarcinoma that is not associated with p53-negative peritoneal and ovarian serous adenocarcinoma within the same patient. Another case in which we suspected multifocal carcinogenesis was case 1. In case 1, the transition between the serous borderline tumor component and the low-grade serous adenocarcinoma component was observed in the ovary. Given that a serous borderline tumor is a well-known precursor of ovarian low-grade serous adenocarcinoma, the histological findings of the ovarian tumor in case 1 are indicative of primary ovarian origin, and there is a significant chance that the coexisting early tubal carcinoma has arisen independently. Further molecular investigations including mutation analysis of genes involved in carcinogenesis of high-grade/low-grade serous adenocarcinomas (e.g., *TP53*, *BRAF*, and *KRAS*), LOH (loss of heterozygosity), and DNA copy number analysis are needed to assess the clonality of these multifocal pelvic carcinomas.

In conclusion, we demonstrated that mucosal carcinomas of the fallopian tube often coexist with the serous subtype of ovarian cancer, but not with clear cell adenocarcinoma and other non-serous adenocarcinomas of the ovary, in the Japanese population. In comparison with previous studies, tubal lesions in our series showed p53 protein overexpression less frequently. We also encountered a rare case of ovarian low-grade serous adenocarcinoma that coexisted with low-grade tubal carcinoma. Mucosal carcinoma of the fallopian tube is certainly a candidate origin (i.e., early manifestation) of ovarian and peritoneal serous carcinomas. However, to truly demonstrate its role as a preceding lesion, there are obstacles to overcome. Our observations indicate the possible heterogeneity of the lesions currently regarded as TICs or mucosal carcinomas of the fallopian tube on a histological basis. In other words, a few of them may represent a part of multiclonal pelvic serous tumors, and a very few others may be cancer dissemination showing tubal intraepithelial spread. We hope that larger studies from around the world will provide fresh and more comprehensive views on this issue. Finally, the fact that about half of the ovarian serous adenocarcinomas do not have coexisting tubal lesions should not be disregarded. At this point, the conventional de novo pathway that considers the origin of serous adenocarcinoma to be in the ovarian surface epithelium cannot be completely eliminated from the list.

Acknowledgements The authors thank the faculty and resident staff in the Department of Pathology at the University of Tokyo Hospital and Mitsui Memorial Hospital, especially Hideki Miyazaki and Masako Ikemura, for their assistance with the extensive sectioning of the fallopian tubes.

Conflict of interest None.

References

1. Seidman JD, Russell P, Kurman RJ (2002) Surface epithelial tumors of the ovary. In: Kurman RJ (ed) Blaustein's pathology of the female genital tract, 5th edn. Springer, New York, pp 873–878
2. Fukunaga M, Nomura K, Ishikawa E et al (1997) Ovarian atypical endometriosis: its close association with malignant epithelial tumours. Histopathology 30:249–255
3. Okuda T, Otsuka J, Sekizawa A et al (2003) p53 mutations and overexpression affect prognosis of ovarian endometrioid cancer but not clear cell cancer. Gynecol Oncol 88:318–325
4. Modesitt SC, Tortolero-Luna G, Robinson JB et al (2002) Ovarian and extraovarian endometriosis-associated cancer. Obstet Gynecol 100:788–795
5. Malpica A (2008) Grading of ovarian cancer: a histotype-specific approach. Int J Gynecol Pathol 27:175–181
6. Shih IM, Kurman RJ (2004) Ovarian tumorigenesis: a proposed model based on morphological and molecular genetic analysis. Am J Pathol 164:1511–1518
7. Lee Y, Medeiros F, Kindelberger D et al (2006) Advances in the recognition of tubal intraepithelial carcinoma: applications to cancer screening and the pathogenesis of ovarian cancer. Adv Anat Pathol 13:1–7
8. Salvador S, Rempel A, Soslow RA et al (2008) Chromosomal instability in fallopian tube precursor lesions of serous carcinoma and frequent monoclonality of synchronous ovarian and fallopian tube mucosal serous carcinoma. Gynecol Oncol 110:408–417
9. Medeiros F, Muto MG, Lee Y et al (2006) The tubal fimbria is a preferred site for early adenocarcinoma in women with familial ovarian cancer syndrome. Am J Surg Pathol 30:230–236
10. Kindelberger DW, Lee Y, Miron A et al (2007) Intraepithelial carcinoma of the fimbria and pelvic serous carcinoma: evidence for a causal relationship. Am J Surg Pathol 31:161–169
11. Lee Y, Miron A, Drapkin R et al (2007) A candidate precursor to serous carcinoma that originates in the distal fallopian tube. J Pathol 211:26–35
12. Crum CP, Drapkin R, Miron A et al (2007) The distal fallopian tube: a new model for pelvic serous carcinogenesis. Curr Opin Obstet Gynecol 19:3–9
13. Jarboe E, Folkins A, Nucci MR et al (2008) Serous carcinogenesis in the fallopian tube: a descriptive classification. Int J Gynecol Pathol 27:1–9
14. Levanon K, Crum C, Drapkin R (2008) New insights into the pathogenesis of serous ovarian cancer and its clinical impact. J Clin Oncol 26:5284–5293
15. Roh MH, Kindelberger D, Crum CP (2009) Serous tubal intraepithelial carcinoma and the dominant ovarian mass: clues to serous tumor origin? Am J Surg Pathol 33:376–383
16. Powell CB, Kenley E, Chen LM et al (2005) Risk-reducing salpingo-oophorectomy in BRCA mutation carriers: role of serial sectioning in the detection of occult malignancy. J Clin Oncol 23:127–132
17. Finch A, Shaw P, Rosen B et al (2006) Clinical and pathologic findings of prophylactic salpingo-oophorectomies in 159 BRCA1 and BRCA2 carriers. Gynecol Oncol 100:58–64
18. Colgan TJ, Murphy J, Cole DE et al (2001) Occult carcinoma in prophylactic oophorectomy specimens: prevalence and association

with BRCA germline mutation status. Am J Surg Pathol 25:1283–1289
19. Sugiyama T, Kamura T, Kigawa J et al (2000) Clinical characteristics of clear cell carcinoma of the ovary: a distinct histologic type with poor prognosis and resistance to platinum-based chemotherapy. Cancer 88:2584–2589
20. Itamochi H, Kigawa J, Terakawa N (2008) Mechanisms of chemoresistance and poor prognosis in ovarian clear cell carcinoma. Cancer Sci 99:653–658
21. Katabuchi H, Takano M, Udagawa Y (2008) Clinical conference: clear cell adenocarcinoma of the ovary. Nippon Sanka Fujinka Gakkai Zasshi 60:224–228
22. Benedet JL, Bender H, Jones H 3rd et al (2000) FIGO staging classifications and clinical practice guidelines in the management of gynecologic cancers. FIGO committee on gynecologic oncology. Int J Gynaecol Obstet 70:209–262
23. Tavassoli FA, Devilee P (eds) (2003) Pathology and genetics of tumours of the breast and female genital organs. IARC Press, Lyon
24. Malpica A, Deavers MT, Lu K et al (2004) Grading ovarian serous carcinoma using a two-tier system. Am J Surg Pathol 28:496–504
25. Anttila MA, Ji H, Juhola MT et al (1999) The prognostic significance of p53 expression quantitated by computerized image analysis in epithelial ovarian cancer. Int J Gynecol Pathol 18:42–51
26. Kobel M, Kalloger SE, Carrick J et al (2009) A limited panel of immunomarkers can reliably distinguish between clear cell and high-grade serous carcinoma of the ovary. Am J Surg Pathol 33:14–21
27. Holstege H, Joose SA, van Oostrom CTM et al (2009) High incidence of protein-truncating TP53 mutations in BRCA1-related breast cancer. Cancer Res 69:3625–3633
28. Shaw PA, Rouzbahman M, Pizer ES et al (2009) Candidate serous cancer precursors in fallopian tube epithelium of BRCA1/2 mutation carriers. Mod Pathol 22:1133–1138
29. Boyd J (2003) Specific keynote: hereditary ovarian cancer: what we know. Gynecol Oncol 88:S8–S10
30. Shaw PA, McLaughlin JR, Zweemer RP et al (2002) Histopathologic features of genetically determined ovarian cancer. Int J Gynecol Pathol 21:407–411
31. Schorge JO, Muto MG, Welch WR et al (1998) Molecular evidence for multifocal papillary serous carcinoma of the peritoneum in patients with germline BRCA1 mutations. J Natl Cancer Inst 90:841–845
32. Maeda D, Takazawa Y, Ota S et al (2010) Bilateral microscopic adenocarcinoma of the fallopian tubes detected by an endometrial cytologic smear. Int J Gynecol Pathol 29:273–277

Oncogene (2010) 29, 5311–5321

www.nature.com/onc

ORIGINAL ARTICLE

The cell polarity regulator hScrib controls ERK activation through a KIM site-dependent interaction

K Nagasaka[1,2], D Pim[1], P Massimi[1], M Thomas[1], V Tomaić[1], VK Subbaiah[1], C Kranjec[1], S Nakagawa[2], T Yano[2], Y Taketani[2], M Myers[1] and L Banks[1]

[1]International Centre for Genetic Engineering and Biotechnology, Area Science Park, Trieste, Italy and [2]Department of Obstetrics and Gynecology, Graduate School of Medicine, University of Tokyo, Tokyo, Japan

The cell polarity regulator, human Scribble (hScrib), is a potential tumour suppressor whose loss is a frequent event in late-stage cancer development. Little is yet known about the mode of action of hScrib, although recent reports suggest its role in the regulation of cell signalling. In this study we show that hScrib is a direct regulator of extracellular signal-regulated kinase (ERK). In human keratinocytes, loss of hScrib results in elevated phospho-ERK levels and concomitant increased nuclear translocation of phospho-ERK. We also show that hScrib interacts with ERK through two well-conserved kinase interaction motif (KIM) docking sites, both of which are also required for ERK-induced phosphorylation of hScrib on two distinct residues. Although wild-type hScrib can down-regulate activation of ERK and oncogenic Ras co-transforming activity, an hScrib mutant that lacks the carboxy terminal KIM docking site has no such effects. These results provide a clear mechanistic explanation of how hScrib can regulate ERK signalling and begin to explain how loss of hScrib during cancer development can contribute to disease progression.
Oncogene (2010) **29,** 5311–5321; doi:10.1038/onc.2010.265; published online 12 July 2010

Keywords: hScrib; phosphorylation; ERK; protein kinase A

Introduction

The mitogen-activated protein kinase (MAPK) pathways that activate extracellular signal-regulated kinase (ERK), c-Jun amino-terminal kinase (JNK) and p38 kinases have important roles in modifying the morphogenetic and motile responses of cells. Among these pathways, the Ras/Raf/MEK/ERK signal transduction cascade is a key mechanism for regulating cell fate in response to growth, proliferation, differentiation and survival signals (Fang and Richardson, 2005; Kolch, 2005; Torii *et al.*, 2006; Yoon and Seger, 2006). Activation of the cascade ultimately results in the activation of ERK and its dissociation from the MEK–ERK complex, which then stimulates gene expression, cytoskeletal rearrangements and cell metabolism, coordinating the cell's responses to a variety of extracellular signals (Schaeffer and Weber, 1999; Fincham *et al.*, 2000). Aberrations in ERK1/2 signalling are also known to be involved in a wide range of pathologies, including many cancers, diabetes, viral infections and cardiovascular disease. This pathway is hyperactivated in many tumours, with activating mutations of Ras occurring in approximately 15–30% of all human cancers (Malumbres and Barbacid, 2003; Garnett *et al.*, 2005).

Recent studies have shown that proteins involved in the regulation of cell polarity can also affect cell signalling cascades. Two of the most well-characterized of these proteins are human discs large (hDlg) and human Scribble (hScrib). In *Drosophila*, these proteins cooperate to regulate pathways of cell polarity and cell proliferation control (Bilder *et al.*, 2000; Bilder, 2004; Zeitler *et al.*, 2004). In humans, the function of these proteins is less clear. However, both are targets for several human tumour viruses and the expression of both hDlg and hScrib is frequently lost during the later stages of malignant progression, suggesting that they possess potential tumour suppressor functions in human cells (Kiyono *et al.*, 1997; Gardiol *et al.*, 1999, 2006; Nakagawa and Huibregtse, 2000; Nakagawa *et al.*, 2004; Navarro *et al.*, 2005; Nagasaka *et al.*, 2006). In the case of hDlg, multiple phosphorylation events by p38γ and JNK have been shown to regulate its localization (Sabio *et al.*, 2005; Massimi *et al.*, 2006) and recent studies have also shown that the entire hScrib cell polarity complex, comprising hDlg, hScrib and Hugl1 (human lethal giant larvae), is dynamically regulated after activation of the MAPK signalling cascade (Massimi *et al.*, 2008). A more direct effect of hScrib on the regulation of this cascade has also been shown. In one study, hScrib was shown to be able to inhibit signalling downstream of Ras and Raf, but upstream of ERK (Dow *et al.*, 2008), with loss of hScrib enhancing Ras-induced cell invasion. In a separate study, hScrib was also shown to be involved in regulating oncogene-induced apoptosis in a JNK-dependent manner, with loss of Scribble cooperating with c-myc in a mouse model of mammary carcinogenesis (Zhan *et al.*, 2008).

Correspondence: Dr L Banks or Dr K Nagasaka, International Centre for Genetic Engineering and Biotechnology, Area Science Park, Padriciano-99, I-34012 Trieste, Italy.
E-mails: banks@icgeb.org or nagasaka@icgeb.org
Received 23 November 2009; revised 21 February 2010; accepted 25 May 2010; published online 12 July 2010

All of the above data indicate that Scribble can act by modulating MAPK signalling and show a clear role for Scribble as a suppressor of tumour invasion. However, in the context of the Ras/Raf/MEK/ERK signalling module, there is no information as to how this is inhibited by Scribble. In this study, we now show that hScrib downregulates ERK activation and inhibits nuclear translocation of activated ERK through a direct protein–protein interaction, thereby providing a direct mechanism for hScrib regulation of the ERK signalling cascade.

Results

Loss of hScrib enhances ERK nuclear localization

Previous studies have shown that loss of hScrib cooperates with activated ras in the induction of invasion in MCF10A cells, an activity that seemed to be related with Scribble's ability to downregulate ERK signalling (Dow *et al.*, 2008). We therefore first wanted to investigate whether hScrib could potentially affect ERK signalling in human keratinocytes. To do this, we generated a series of HaCaT cell lines in which hScrib levels had been ablated using short hairpin RNA targeting vectors (Massimi *et al.*, 2008). Cells were then either left untreated or exposed to osmotic shock for 30 min to enhance ERK activation. The cells were then extracted and the levels of hScrib, total ERK and activated phospho-ERK were monitored by western blotting. The results in Figure 1a show a modest level of constitutively active ERK in HaCaT cells. However, in the hScrib knockdown cells there is a marked increase in the levels of phospho-ERK in both cell lines and this increases further after osmotic shock. These results show that hScrib can contribute to the regulation of the ERK signalling cascade in human keratinocytes.

Activated ERK has been shown to translocate to the nucleus (Chen *et al.*, 1992; Gonzalez *et al.*, 1993; Lenormand *et al.*, 1993; Treisman, 1996; Fukuda *et al.*, 1997; Khokhlatchev *et al.*, 1998; Pouyssegur *et al.*, 2002). We therefore investigated whether there was a change in the pattern of ERK localization in HaCaT cells when hScrib expression levels were reduced. To do this, immunofluorescence analysis of total and phospho-ERK expression was carried out on the control and shScrib cell lines, and the results obtained are shown in Figure 1b. As can be seen, loss of hScrib (Figure 1biii) also results in a significant increase in the amount of nuclear-translocated ERK. In contrast, activated ERK seems to accumulate in Golgi-like structures in the cytoplasm of the control cells (Figures 1bi and bii), consistent with previous reports (Torii *et al.*, 2004). To verify these results, we also performed a series of transient small interfering RNA experiments, in which hScrib levels were ablated in HEK293 cells, and the levels of phospho-ERK in both total cell extracts (Figure 2a) or in the respective cellular fractions (Figure 2b) were analysed by western blotting. In both cases, loss of hScrib enhanced ERK activation and also resulted in enhanced nuclear accumulation of active phospho-ERK. These results show that one consequence of hScrib knockdown is enhanced nuclear translocation of activated ERK.

hScrib is a substrate of ERK and PKA

Having confirmed that hScrib could regulate ERK activation and nuclear translocation, we next wanted to investigate the mechanism by which this might occur. Analysis of the hScrib sequence revealed the presence of two perfect ERK-binding sites (kinase interaction motif (KIM) sites) at positions 836aa–846aa and 1396aa–1404aa (Figure 3). In addition, two potential ERK phospho-acceptor sites are correspondingly located at residues S853 and S1448, downstream of each of the two KIM sites (Figure 3).

To first investigate whether either of these two potential phospho-acceptor sites on hScrib was phosphorylated *in vivo*, we transfected cells with hemagglutinin (HA)-tagged hScrib expression plasmid and grew the cells with or without osmotic shock. The cells were then extracted, and hScrib protein was immunoprecipitated with anti-HA agarose beads. The subsequently gel-purified protein was then subjected to mass spectroscopy analysis. A summary of the phospho-peptides that were identified under the two culture conditions is shown in Figure 3. As can be seen, the N-terminal site at position S853 is phosphorylated in unstressed conditions, as is S1445 in the carboxy terminal region of the protein. Interestingly, after exposure to osmotic shock, S853 remains phosphorylated, whereas S1445 is no longer phosphorylated and the phosphorylation event occurs exclusively on S1448, just three amino acids downstream. These results show clear differential phosphorylation of hScrib *in vivo*, both before and after osmotic stress.

On the basis of these data we reasoned that ERK was a prime candidate kinase for the phosphorylation events at S853 and S1448, with the corresponding upstream KIM sites located approximately at residues 836 and 1396, respectively, whereas the phospho-site at S1445 corresponds to a potential PKA recognition site. To first confirm whether these were the responsible kinases, we analysed whether hScrib was a substrate for ERK and PKA *in vitro*. To do this, a glutathione *S*-transferase (GST)–hScrib fusion protein was purified and incubated with the purified recombinant kinases and [γ^{32}P]-ATP, and the results obtained are shown in Figure 4a. As can be seen, GST–hScrib is a good substrate for phosphorylation by both PKA and ERK1, and is only a very weak substrate for JNK and ERK2. To then determine whether the putative KIM and phospho-acceptor sites on hScrib corresponded to those identified *in vivo*, we generated a series of GST–hScrib fusion proteins that had been mutated in both the ERK KIM recognition sites, the two potential ERK phospho-acceptor sites and in the potential PKA phospho-acceptor site (Figure 4b). The purified GST proteins were then incubated with the purified kinases and [γ^{32}P]-ATP, and the results obtained are shown in Figure 4c. As can be seen, the PKA phospho-acceptor site on

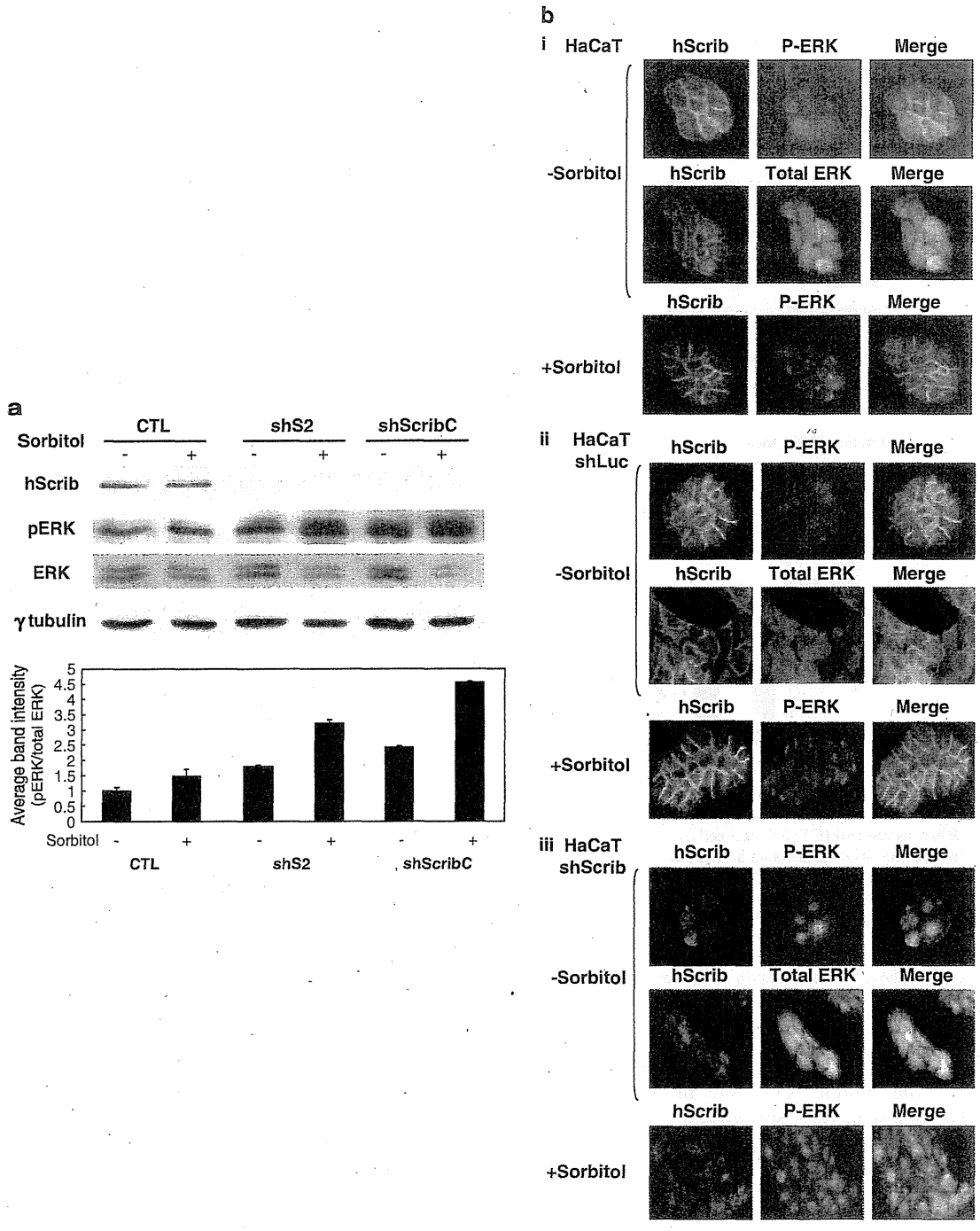

Figure 1 hScrib suppresses/downregulates the Raf/MEK/ERK pathway. (**a**) The sh-hScrib stable cell lines (S2, ScribC) and control cells (CTL) were cultured overnight and either left untreated or exposed to sorbitol for 30 min as indicated. The cells were then harvested and levels of ERK, phospho-ERK and hScrib were analysed by western blotting. γ-Tubulin was used as a loading control. The lower histogram shows the quantitative analyses of the intensities of the pERK bands from three independent experiments with s.d. indicated. (**b**) Immunofluorescent analysis of hScrib and ERK expression. HaCaT cells (i), sh-Luc control TR cells (ii) and sh-hScrib cells (iii) were grown on coverslips and then exposed to sorbitol as indicated. The cells were then fixed and double stained with the anti-hScrib antibody, the anti-phospho-ERK1/2 antibody or the anti-total ERK1/2 antibody.

GST–hScrib maps precisely to residue S1445 identified in the mass spectroscopic analysis. In the case of ERK1 the results are more complex. First, there are clearly two phospho-acceptor sites, at S853 and S1448, again corresponding to the two sites that were identified *in vivo*. Both KIM sites seem to be important for ERK1 recognition, with mutation of either site decreasing the phosphorylation to a level equivalent to that observed

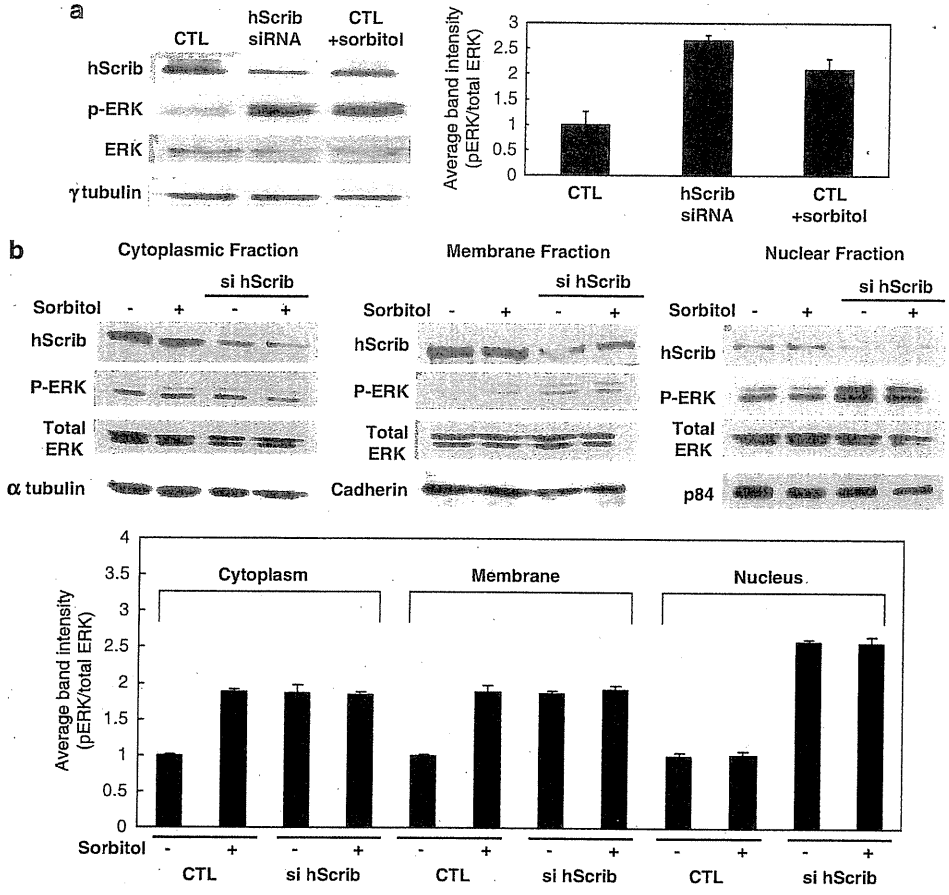

Figure 2 Loss of hScrib enhances phospho-ERK nuclear translocation. (**a**) HEK293 cells were transfected with hScrib siRNA and siLuc RNA as control (CTL). Total cell extracts were then made after 48 h, and hScrib, pERK, ERK and γ-tubulin were detected by western blotting. The right-hand histogram shows the quantitative changes in phospho-ERK/total ERK levels from a minimum of three independent assays. (**b**) HEK293 cells were transfected with hScrib siRNA and siLuc RNA as control, and then exposed to sorbitol for 20 min as indicated. Cells were fractionated into cytoplasmic, membrane and nuclear pools then phospho-ERK was then detected by western blotting. p84 was used as a loading control for the nuclear fraction, E-cadherin was used as a loading control for the membrane fraction and α-tubulin was used as the loading control for the cytoplasmic fraction. The lower histogram shows the quantitative changes in phospho-ERK/total ERK levels from a minimum of three independent assays. Note the relative increase in nuclear phospho-ERK after hScrib knockdown.

with the respective single phospho-site mutations. Most importantly, the double KIM site mutations, or the double phospho-acceptor site mutations, completely abolish ERK phosphorylation of hScrib (Figure 4c). In contrast, all of these mutants are still recognized by PKA (Figure 4d), showing that these mutations do not overly perturb the overall structure of hScrib, and further show the specificity of the assays. These results show that hScrib has two ERK docking sites and two corresponding phospho-acceptor sites, with S853 phosphorylated under normal growth conditions and S1448 being phosphorylated under conditions of osmotic stress.

hScrib regulates ERK activation through the two KIM docking sites

We next wanted to investigate whether the two identified KIM sites could actually serve as docking sites for ERK *in vitro* and *in vivo*. The GST–hScrib fusion proteins were first used in pull-down assays using the commercially purified ERK1, and levels of bound ERK1 were assessed by western blotting. The results obtained are shown in Figure 5a and show a strong direct interaction between the wild-type hScrib and ERK1. In contrast, mutation of the C-terminal KIM site largely abolishes the interaction, showing that most of the interaction is through this carboxy terminal site, although a weaker interaction is also mediated by the N-terminal KIM site. To investigate whether these sites on hScrib were also responsible for ERK binding *in vivo*, we first used the GST–hScrib fusion proteins to pull down ERK from cell extracts and then analysed by western blotting for total and phospho-ERK. The results obtained are shown in Figure 5b. As can be seen, the two KIM sites contribute to hScrib binding to ERK, although the C-terminal site seems to be the strongest site of interaction, with mutation of this single site almost abolishing ERK

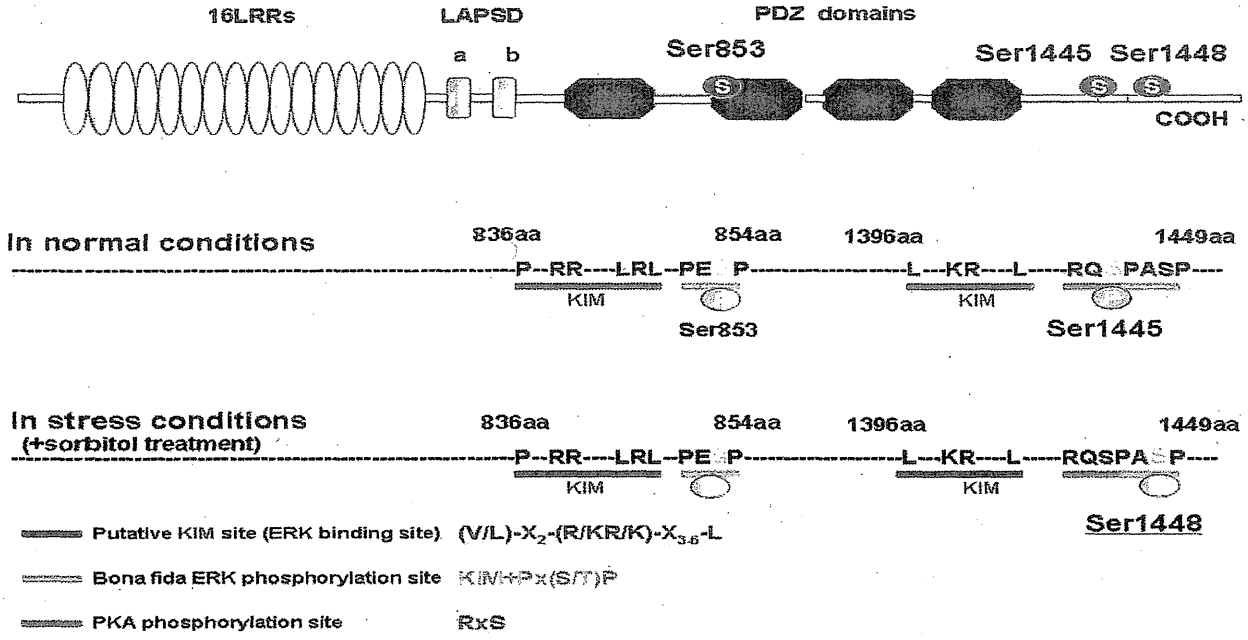

Figure 3 Identification of hScrib phospho-acceptor sites. Lysates from HEK293 cells transfected with HA-tagged hScrib either in the absence (−) or presence (+) of sorbitol for 30 min were subjected to immunoprecipitation with an anti-HA antibody. Complexes were run on SDS–PAGE and the hScrib gel slice was then subjected to mass spectrometry. Residues at S853, S1445 and S1448 were identified as phospho sites. The consensus ERK-phosphorylation motif (PESP, PASP), the consensus PKA-phosphorylation motif (RXS) (Pearson and Kemp, 1991) and the putative ERK docking site or a kinase interaction motif ((V/L)-X_2-(R/K)-(R/K)-X_{3-6}-L) (MacKenzie *et al*., 2000; Tanoue *et al*., 2000; Fantz *et al*., 2001; Zhou *et al*., 2006) are shown, in which X is any amino acid.

binding. Interestingly, when extracts are made from cells exposed to osmotic stress, there is a marked increase in the amount of ERK complexed with hScrib, suggesting that ERK activation can enhance its interaction with hScrib. We also carried out co-immunoprecipitation experiments in which HA-tagged wild-type and the ΔKIM mutant of hScrib were transfected into HEK293 cells, and then immunoprecipitated with anti-HA agarose beads. The co-precipitated ERK was then detected by western blotting. The results in Figure 5c also show that hScrib binds ERK *in vivo* in a KIM site-dependent manner and, in addition, this interaction also seems to be enhanced when the cells are exposed to osmotic stress.

The above results show that loss of hScrib enhances ERK activation and that hScrib can interact with ERK through two KIM docking sites. We next wanted to investigate whether the ability of hScrib to directly interact with ERK was responsible for its ability to downregulate ERK activation. To do this, HEK293 cells were transfected with the wild-type hScrib and the ΔKIM mutants. After 24 h, the cells were extracted and the levels of activated phospho-ERK were analysed by western blotting. The results obtained are shown in Figure 6 and show a clear downregulation in the levels of phospho-ERK when wild-type hScrib is overexpressed. In contrast, the hScrib that has the carboxy terminal KIM site mutation is no longer capable of affecting the levels of ERK phosphorylation, whereas the amino terminal KIM site mutant can downregulate phospho-ERK to levels close to those obtained with the wild-type hScrib. These results show that hScrib can directly regulate the levels of ERK activation through a direct protein–protein interaction with ERK.

To determine whether hScrib downregulation of ERK activation was physiologically relevant, we analysed the effects of the wild-type and non-ERK binding mutant of hScrib in an oncogene cooperation assay. Primary baby rat kidney (BRK) cells were transfected with human papillomavirus-16 E7 plus EJ-ras, in the presence or absence of the hScrib-expressing plasmids. After 3 weeks, the cells were fixed and stained and the numbers of colonies counted. The results obtained are shown in Figure 7 and Table 1. As can be seen, wild-type hScrib can inhibit the oncogene cooperation between E7 and EJ-ras, whereas a non-ERK binding mutant of hScrib is compromised in this activity. These results show that hScrib binding to ERK is functionally relevant in an assay of oncogene cooperation.

Discussion

Previous studies have reported many diverse functions for the hScrib protein. These include regulation of cell proliferation, cell polarity, cell migration and cell invasion in a variety of different cell types. Perhaps the most intriguing of these observations are the demonstrations that hScrib can potentially regulate MAPK signalling. Loss of hScrib was reported to enhance cell survival by inhibiting JNK-induced apoptosis in mammary tumour models of oncogene-induced

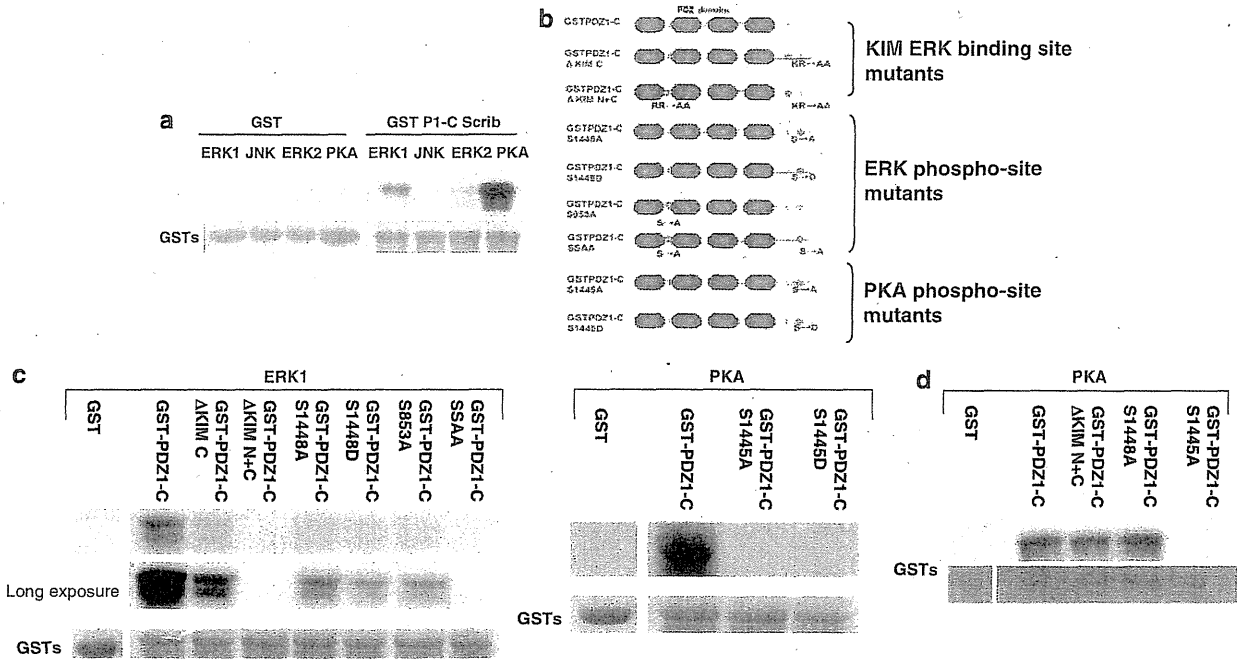

Figure 4 hScrib is a substrate for ERK1 and PKA. (**a**) The GST–hScrib fusion protein PDZ1-C (P1-C hScrib) and GST alone were incubated with purified ERK1, ERK2, JNK and PKA together with radiolabel, and after 20 min the level of phosphorylation was ascertained by SDS–PAGE and autoradiography (upper panels). The lower panels show the Coomassie protein stain of the gels. (**b**) A panel of hScrib mutants in which the ERK consensus phospho-acceptor sites (1448 and 853) and the PKA phospho-acceptor site (1445) were substituted with alanine or aspartic acid either individually or in combination. The ERK docking KIM sites (836 and 1396) sites were similarly either singly KR/AA (C terminal; ΔKIM C) or doubly RR/AA:KR/AA (N-terminal and C-terminal; ΔKIM N + C) mutated. (**c**) The wild-type and mutant hScrib fusion proteins with GST as control, were subjected to *in vitro* phosphorylation assays with ERK1 (left) or PKA (right) and then analysed by SDS–PAGE and autoradiography. The bottom panels show the Coomassie protein stains of the gels. (**d**) The wild-type and mutant hScrib fusion proteins defective in ERK1 recognition were subjected to *in vitro* phosphorylation assays with PKA and then analysed by SDS–PAGE and autoradiography. The bottom panel shows the Coomassie protein stain of the gel.

carcinogenesis (Zhan *et al.*, 2008). hScrib was also reported to act upstream of ERK in the Ras/Raf/MEK/ERK signalling cascade to inhibit ERK activation and suppress Ras-induced cell invasion in breast epithelial cells (Dow *et al.*, 2008). In this study, we show that hScrib regulates the ERK signalling pathway in human keratinocytes through a direct protein interaction with ERK. The consequences of this are inhibition of ERK phosphorylation and subsequent inhibition of ERK nuclear translocation.

In human skin keratinocytes, we observed that loss of hScrib expression induces an upregulation in the levels of activated phospho-ERK, providing the first indication that hScrib might also regulate ERK signalling in these cells. Most interestingly, loss of hScrib expression is accompanied by a marked accumulation of active phospho-ERK in the Golgi apparatus and in the nucleus. Although nuclear localized ERK is most likely involved in the regulation of gene expression related to cell cycle progression, Golgi accumulation may be related to the control of cell survival and cell migration, both of which have also been shown to be regulated by hScrib (Qin *et al.*, 2005; Dow *et al.*, 2008; Nola *et al.*, 2008).

An understanding of how hScrib directly regulates ERK function has come from the identification of two ERK docking sites on hScrib. These two KIM sites are found at N- and C-terminal locations on hScrib, and both are essential for directing the interaction between ERK and hScrib, but with the C-terminal site having the strongest affinity for ERK. One of the most likely consequences of this interaction is to inhibit ERK translocation to the nucleus. However, an additional important feature is the direct inhibition of ERK activation as a result of the ability of hScrib to bind ERK. The mechanism by which this is achieved remains to be determined, although recruitment of de-activating phosphatases to the complex remains an intriguing possibility.

During the course of this analysis, we mapped three phospho-acceptor sites on hScrib. Under normal growth conditions, hScrib is phosphorylated at S853, most likely by ERK, and at S1445 by PKA. Interestingly, stimulation of MAPK by osmotic stress results in a marked loss of phosphorylation at the PKA site S1445, but a concomitant increase in phosphorylation at S1448, presumably also by ERK. Previous studies have shown that PKA phosphorylation close to a KIM site might inhibit ERK binding (Houslay and Kolch, 2000), although at present we do not know whether PKA phosphorylation can similarly affect the ability of hScrib to interact with ERK. ERK1 (p44) and ERK2 (p42)

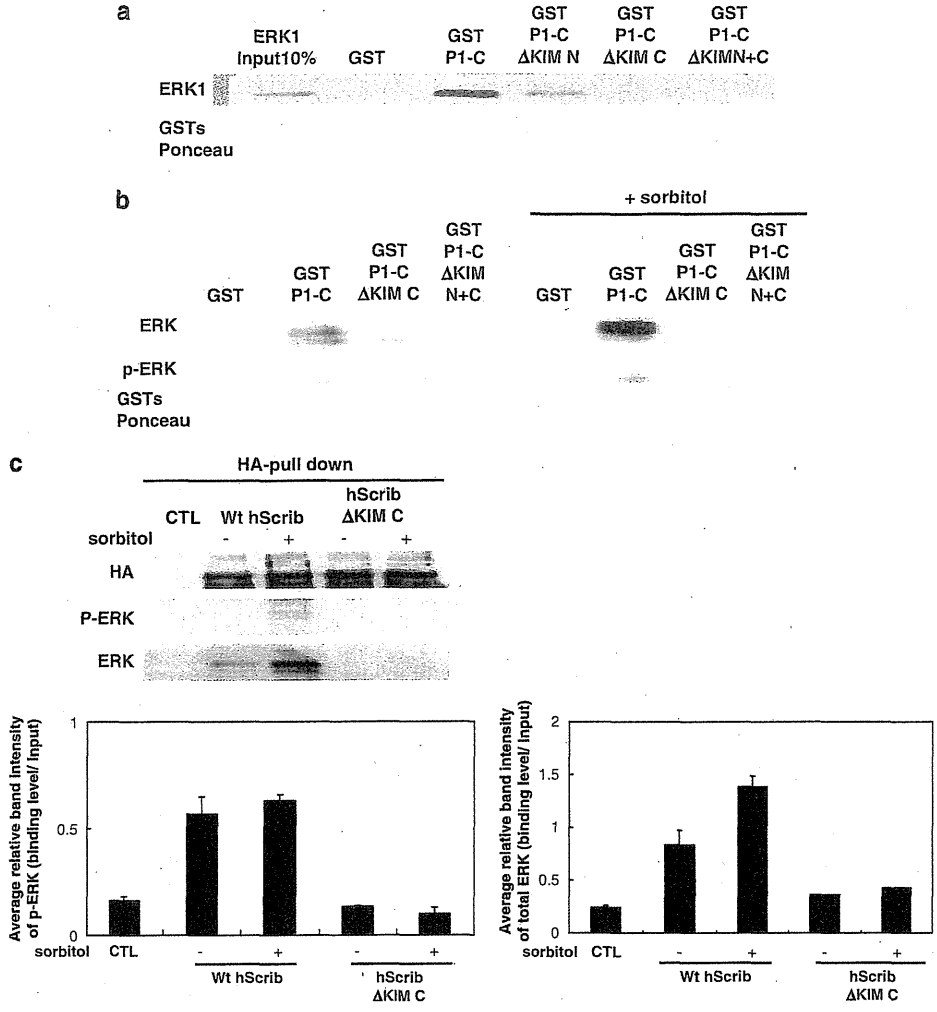

Figure 5 hScrib interacts directly with ERK through the two KIM sites. (**a**) Commercially available purified ERK1 was incubated with the GST-PDZ1-C wild-type and the ΔKIM N, ΔKIM C and the ΔKIM N + C mutants and bound ERK1 ascertained by western blotting. The lower panel shows the Ponceau stain of the nitrocellulose membrane. (**b**) HEK293 cell extracts from untreated and sorbitol-exposed cells were incubated with the GST-PDZ1-C wild-type and the two KIM site mutant GST fusion proteins (single and double) immobilized on glutathione-agarose beads. The bound proteins were analysed by western blotting with the anti-phospho ERK1/2 antibody and the anti-ERK1/2 antibody. The input GSTs are shown in the Ponceau stain of the nitrocellulose membrane. (**c**) HEK293 cells transfected with pcDNA3.1 (CTL), HA-hScrib or the HA-hScribΔKIM C mutant and the cells were then either incubated with or without 0.3 M sorbitol for 10 min, after which the cells were extracted and immunoprecipitated with anti-HA agarose beads. Co-immunoprecipitated proteins were then analysed by western blotting for anti HA-Scrib and anti-pERK/total ERK. The lower histogram shows the quantitative analyses of the intensities of the pERK and total ERK bindings from three independent experiments with s.d. indicated.

have numerous substrates in common, many of which are nuclear and which participate in the transcriptional regulation of a number of different cellular processes (Treisman, 1996). However, ERK1 and ERK2 are not entirely functionally redundant, and our studies confirm this as we found that hScrib S1448 is preferentially phosphorylated by ERK1. At present, we have no information as to what are the functional consequences of ERK or PKA phosphorylation of hScrib. However, we can speculate that this will most likely affect the ability of hScrib to interact with some of its cellular partners, and studies are currently in progress to investigate these aspects further.

Finally, it is worth noting that only in *Homo sapiens* is the organization of the two KIM sites and the corresponding phospho-acceptor sites perfectly well conserved in Scribble. Figure 8 shows the sequence alignment of Scribble from a number of different organisms. It can be seen from this that although the C-terminal KIM and phospho-acceptor site are well conserved among vertebrate species, the N-terminal site is somewhat divergent, whereas in lower organisms neither of the two regulatory elements seem to be conserved. This is particularly true for *Drosophila*, which has been the model organism of choice for many of the studies on hScrib, and suggests a very different

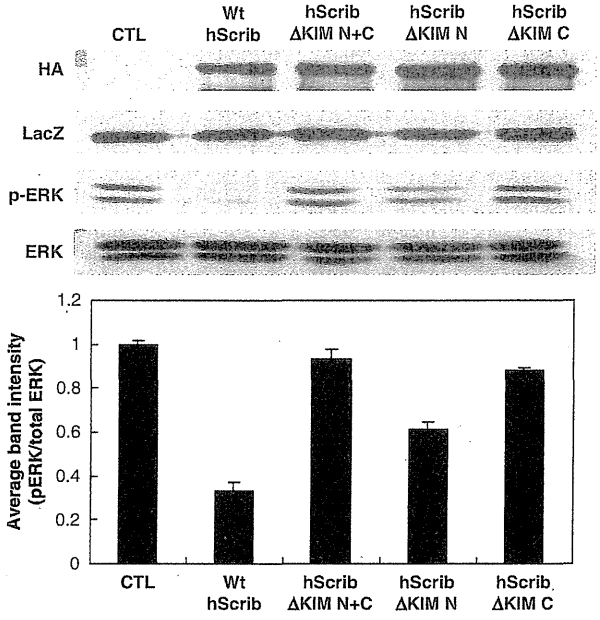

Figure 6 hScrib downregulates ERK activation through a direct interaction. HEK293 cells were transfected with pcDNA3.1 (CTL), HA-tagged wild-type hScrib, ΔKIM N + C, ΔKIM N and ΔKIM C mutants. After 24 h, the cells were harvested and the levels of ERK and phospho-ERK were analysed by western blotting. LacZ was monitored as a control for transfection efficiency. The lower panel shows the quantifications of the pERK/total ERK ratios from at least three independent experiments.

form of regulation and function of hScrib between flies and higher organisms. It is also worth noting that only in *Homo sapiens* is the potential regulatory PKA site so closely juxtaposed to the carboxy terminal ERK phospho-acceptor site, and further studies are warranted to determine whether there are any co-regulatory effects in humans of these two kinases on hScrib.

In summary, we have identified a novel regulatory mechanism by which the cell polarity regulator hScrib can directly control the MAPK signalling cascade through a direct protein interaction with ERK. These studies suggest that loss of hScrib expression, which is observed in many tumours, can directly affect continued cell proliferation and cell survival by increasing MAPK activation and nuclear translocation.

Materials and methods

Cells and treatments

HEK293 (human embryonic kidney cells), HaCaT (human keratinocyte) and BRK cells were cultured in Dulbecco's modified Eagles's medium supplemented with 10% fetal bovine serum, penicillin–streptomycin (100 U/ml) and glutamine (300 μg/ml) in a humidified 5% CO_2 incubator. Transfection was carried out using calcium phosphate precipitation as described previously (Graham and van der Eb, 1973) or using Lipofectamine 2000 (Invitrogen, Milan, Italy) according to the manufacturer's protocol. To generate the depleted Scribble cell lines, HaCaT cells were transfected using a pool of short hairpin RNA constructs against hScrib (S2, ScribC) using Lipofectamine 2000 (Invitrogen). The cells were then selected with puromycin (500 ng/ml) and after 4 weeks single colonies were analysed for hScrib expression by immunofluorescence and western blotting, and two such separate colonies (S2, ScribC) were used in this analysis. Parallel transfections and selections were performed using empty vector to generate control clones (TR) that had been subjected to the drug selection. For induction of osmotic shock, the cells were exposed to 0.3 M sorbitol for the times indicated in the text.

Cell transformation assays were performed using BRK cells obtained from 9-day-old Wistar rats with a combination of human papillomavirus-16 E7 and EJ-ras plus the appropriate hScrib expression plasmids. Cells were placed under G418 selection for 3 weeks, and then fixed and stained as described previously (Thomas *et al*., 2005).

Plasmids

The wild-type HA-tagged pcDNA hScrib expression plasmid and the truncated mutant pGEX hScrib PDZ1-C, PDZ1-4

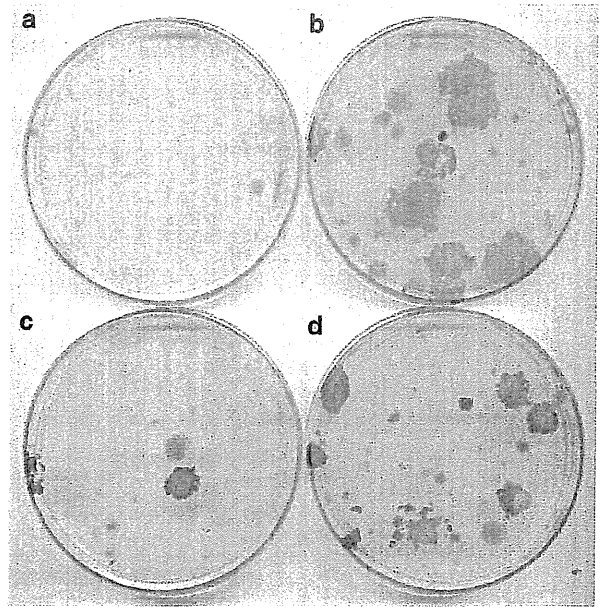

Figure 7 hScrib suppresses human papillomavirus (HPV)-16 E7 and EJ-ras oncogene cooperation in a KIM site-dependent manner. BRK cells were transfected with EJ-ras alone (**a**), HPV-16 E7 plus EJ-ras (**b**), HPV-16 E7 plus EJ-ras and wild-type hScrib (**c**) and HPV-16 E7 plus EJ-ras and the ΔKIM C hScrib mutant (**d**). After 3 weeks, the dishes were fixed and stained and the colonies counted.

Table 1 Suppression of HPV-16 E7 and EJ-ras cooperation by hScrib is KIM site-dependent

	Number of cell colonies		
	Exp 1	*Exp 2*	*Exp 3*
EJ-ras	10	0	0
EJ-ras + 16 E7	52	34	63
EJ-ras + 16 E7 + hScrib	22	11	44
EJ-ras + 16 E7 + hScrib ΔKIMC	30	33	59

Abbreviations: HPV, human papillomavirus; hScrib, human Scribble; KIM, kinase interaction motif; KIM C, KIM C-terminal.
Number of colonies obtained after 3 weeks of cultivation in three independent assays.

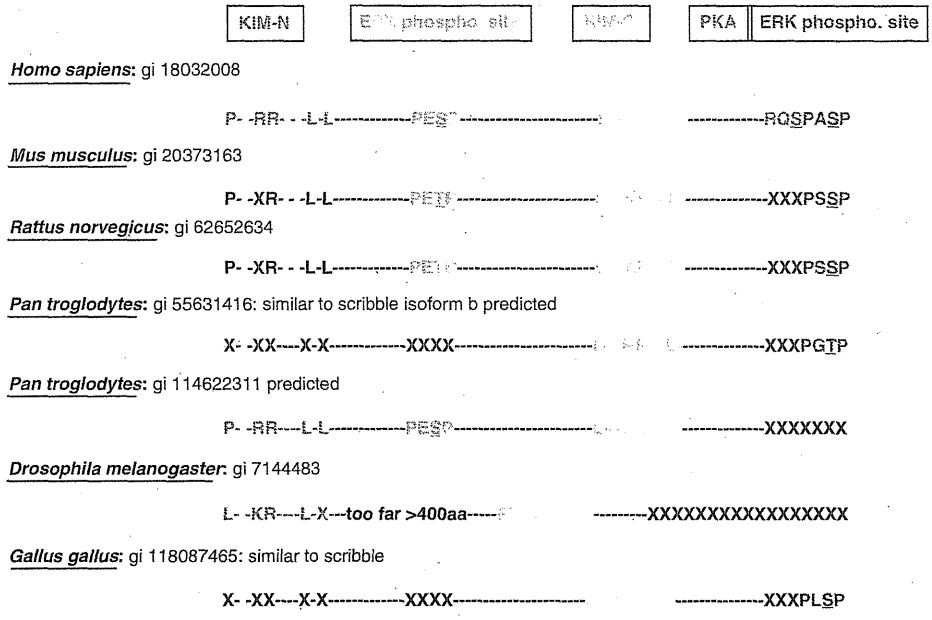

Figure 8 Comparison and sequence alignment of the region of hScrib containing the consensus ERK phosphorylation/binding sites in humans, chimpanzees, mice, rats, chickens and *Drosophila*. There is no evidence for the conservation of the C-terminal hScrib-dependent ERK signalling cascade in non-vertebrate species; however, interestingly, only human Scribble has the two ERK sites.

expression plasmids have been described previously (Thomas *et al*., 2005; Nagasaka *et al*., 2006). The mutations of Ser 853, 1445 and 1448 to either singly, doubly alanine(A) or aspartate(D) or KR, RR to alanine AA mutants in hScrib were performed using the QuikChange XL site-directed mutagenesis kit from Stratagene Cloning Systems (La Jolla, CA, USA) (Celbio, Milan, Italy) according to the manufacturer's instruction. The mutants were confirmed by DNA sequencing.

Antibodies

The following commercial antibodies were used at the dilution indicated: anti-hScrib goat polyclonal antibody (Santa Cruz, Santa Cruz, CA, USA; western blot (WB) 1:1000), anti-p44/42 MAPK (Erk1/2) antibody (Cell Signalling Technology, Danvers, MA, USA; WB 1:1000), anti-phospho p44/42 MAPK (Erk1/2) (Thr202/Tyr204) antibody (Cell Signaling Technology, WB 1:1000), anti-HA monoclonal antibody 12CA5 (Roche, Milan, Italy; WB 1:500), anti-β-galactosidase antibody (Promega, Milan, Italy; WB 1:5000), anti-γ-tubulin monoclonal antibody (Sigma, Milan, Italy; WB 1:5000), anti-p84 mouse monoclonal antibody (Abcam, Cambridge, UK; WB 1:1000), anti-α-tubulin mouse monoclonal antibody (Abcam, WB 1:1000) and anti-E-Cadherin rabbit polyclonal antibody (Santa Cruz, WB 1:500).

Immunofluorescence and microscopy

For immunofluorescence, cells were grown on glass coverslips and fixed in 3.7% paraformaldehyde in phosphate-buffered saline (PBS) for 20 min at room temperature. After washing in PBS, the cells were permeabilized in PBS/0.1% Triton for 5 min, washed extensively in PBS and then incubated with primary antibody diluted in PBS for 1 h followed by the appropriately conjugated secondary antibodies. Secondary antibodies conjugated to Alexa Fluor 488 or 548 were obtained from Invitrogen. The cells were then washed several times in water and mounted on glass slides. Cells were visualized using a Zeiss Axiovert 100 M microscope (Zeiss, Milan, Italy) attached to a LSM 510 confocal unit.

Small interfering RNA transfection

HEK293 cells were seeded on 6 cm dishes and transfected using Lipofectamine 2000 (Invitrogen) with control small interfering RNA against Luciferase (siLuc), or small interfering RNA against hScrib sequences (Dharmacon, Lafayette, CO, USA). At 48 h after transfection, cells were harvested and total cells extracts or cell fractionated extracts were then analysed by western blotting.

In vitro *kinase assays*

Purified GST fusion proteins were incubated with commercially purified ERK1, ERK2, JNK1 (Cell Signaling Technology) or PKA (Promega) for 20 min at 30 °C in phosphorylation buffer (0.25 M Tris pH 7.5, 1 M $MgCl_2$, 3 M NaCl, 0.3 mM aprotinin and 1 mM Pepstatin) supplemented with 56 nM [^{32}P] γ-ATP (Perkin Elmer, Waltham, MA, USA) and 10 mM ATP following the manufacturer's instruction. After extensive washing, the phosphorylated proteins were monitored by sodium dodecyl sulphate–polyacrylamide gel electrophoresis (SDS–PAGE) and autoradiography.

Phospho-mapping analyses

HEK293 cells were transfected with HA-tagged Scrib and after 24 h left untreated or exposed to sorbitol for 30 min. After this time, the cells were extracted and proteins immunoprecipitated with anti-HA agarose beads, separated on SDS–PAGE and the silver-stained gel slice corresponding to hScrib was excised. Phospho-mapping mass spectroscopy was then performed using NextGen Sciences (Ann Arbor, MI, USA).

Subcellular fractionation assays

Differential extraction of HEK293 cells to obtain cytoplasmic, nuclear and membrane fractions was performed using the

Calbiochem ProteoExtract Fractionation Kit (Calbiochem, Milan, Italy) according to the manufacturer's instructions. To inhibit phosphatase activity during the preparation of cell lysates, phosphatase inhibitors (1 mM Na_3VO_4, 1 mM β-glycerophosphate, 2.5 mM sodium pyrophosphate and 1 mM sodium fluoride) were also included.

Immunoprecipitation and western blotting

Total cellular extracts were prepared by directly lysing cells from dishes in SDS lysis buffer. Alternatively, cells were lysed in either E1A buffer (25 mM HEPES pH 7.0, 0.1% NP-40, 150 mM NaCl, plus protease inhibitor cocktail; Calbiochem) or RIPA buffer (50 mM Tris–HCl pH 7.4, 1% NP-40, 150 mM NaCl, 1 mM EDTA, plus protease inhibitor cocktail; Calbiochem). The supernatant (soluble fraction), pellet (insoluble fraction) and the whole cells extracts were analysed by SDS–PAGE and western blotting. For immunoprecipitations, total cell lysates were transferred into a tube of equilibrated EZview Red Anti-HA Affinity Gel beads (Sigma), and incubated for 2 h at 4 °C. Immunoprecipitates were extensively washed four times in lysis buffer and solubilized in SDS–PAGE sample buffer. For western blotting, 0.45 μm nitrocellulose membrane (Schleicher and Schuell, Milan, Italy) was used and membranes were blocked for 1 h at 37 °C in 10% milk/PBS followed by incubation with the appropriate primary antibody diluted in 10% milk/0.5% Tween 20 for 1 h. After several washings with PBS 0.5% Tween 20, secondary antibodies conjugated with horseradish peroxidase (DAKO, Milan, Italy) in 10% milk/0.5% Tween 20 were incubated for 1 h. Blots were developed using Amersham enhanced chemiluminescence reagents (Amersham, Milan, Italy) according to the manufacturer's instructions.

Conflict of interest

The authors declare no conflict of interest.

Acknowledgements

This work was supported by the Yoshida (YKK) Scholarship Foundation (to KN) and by a research grant from the Associazione Italiana per la Ricerca sul Cancro (to LB). We are also very grateful to David Allen (Nextgen Sciences) for his kind support and advice on the phospho-mapping analyses.

References

Bilder D. (2004). Epithelial polarity and proliferation control: links from the Drosophila neoplastic tumor suppressors. *Genes Dev* **18**: 1909–1925.

Bilder D, Li M, Perrimon N. (2000). Cooperative regulation of cell polarity and growth by Drosophila tumor suppressors. *Science* **289**: 113–116.

Chen RH, Sarnecki C, Blenis J. (1992). Nuclear localization and regulation of erk- and rsk-encoded protein kinases. *Mol Cell Biol* **12**: 915–927.

Dow LE, Elsum IA, King CL, Kinross KM, Richardson HE, Humbert PO. (2008). Loss of human Scribble cooperates with H-Ras to promote cell invasion through deregulation of MAPK signalling. *Oncogene* **27**: 5988–6001.

Fang JY, Richardson BC. (2005). The MAPK signalling pathways and colorectal cancer. *Lancet Oncol* **6**: 322–327.

Fantz DA, Jacobs D, Glossip D, Kornfeld K. (2001). Docking sites on substrate proteins direct extracellular signal-regulated kinase to phosphorylate specific residues. *J Biol Chem* **276**: 27256–27265.

Fincham VJ, James M, Frame MC, Winder SJ. (2000). Active ERK/MAP kinase is targeted to newly forming cell-matrix adhesions by integrin engagement and v-Src. *EMBO J* **19**: 2911–2923.

Fukuda M, Gotoh Y, Nishida E. (1997). Interaction of MAP kinase with MAP kinase kinase: its possible role in the control of nucleocytoplasmic transport of MAP kinase. *EMBO J* **16**: 1901–1908.

Gardiol D, Kuhne C, Glaunsinger B, Lee SS, Javier R, Banks L. (1999). Oncogenic human papillomavirus E6 proteins target the discs large tumour suppressor for proteasome-mediated degradation. *Oncogene* **18**: 5487–5496.

Gardiol D, Zacchi A, Petrera F, Stanta G, Banks L. (2006). Human discs large and scrib are localized at the same regions in colon mucosa and changes in their expression patterns are correlated with loss of tissue architecture during malignant progression. *Int J Cancer* **119**: 1285–1290.

Garnett MJ, Rana S, Paterson H, Barford D, Marais R. (2005). Wild-type and mutant B-RAF activate C-RAF through distinct mechanisms involving heterodimerization. *Mol Cell* **20**: 963–969.

Gonzalez FA, Seth A, Raden DL, Bowman DS, Fay FS, Davis RJ. (1993). Serum-induced translocation of mitogen-activated protein kinase to the cell surface ruffling membrane and the nucleus. *J Cell Biol* **122**: 1089–1101.

Graham FL, van der Eb AJ. (1973). A new technique for the assay of infectivity of human adenovirus 5 DNA. *Virology* **52**: 456–467.

Houslay MD, Kolch W. (2000). Cell-type specific integration of cross-talk between extracellular signal-regulated kinase and cAMP signaling. *Mol Pharmacol* **58**: 659–668.

Khokhlatchev AV, Canagarajah B, Wilsbacher J, Robinson M, Atkinson M, Goldsmith E *et al.* (1998). Phosphorylation of the MAP kinase ERK2 promotes its homodimerization and nuclear translocation. *Cell* **93**: 605–615.

Kiyono T, Hiraiwa A, Fujita M, Hayashi Y, Akiyama T, Ishibashi M. (1997). Binding of high-risk human papillomavirus E6 oncoproteins to the human homologue of the Drosophila discs large tumor suppressor protein. *Proc Natl Acad Sci USA* **94**: 11612–11616.

Kolch W. (2005). Coordinating ERK/MAPK signalling through scaffolds and inhibitors. *Nat Rev Mol Cell Biol* **6**: 827–837.

Lenormand P, Sardet C, Pages G, L'Allemain G, Brunet A, Pouyssegur J. (1993). Growth factors induce nuclear translocation of MAP kinases (p42mapk and p44mapk) but not of their activator MAP kinase kinase (p45mapkk) in fibroblasts. *J Cell Biol* **122**: 1079–1088.

MacKenzie SJ, Baillie GS, McPhee I, Bolger GB, Houslay MD. (2000). ERK2 mitogen-activated protein kinase binding, phosphorylation, and regulation of the PDE4D cAMP-specific phosphodiesterases. The involvement of COOH-terminal docking sites and NH2-terminal UCR regions. *J Biol Chem* **275**: 16609–16617.

Malumbres M, Barbacid M. (2003). RAS oncogenes: the first 30 years. *Nat Rev Cancer* **3**: 459–465.

Massimi P, Narayan N, Cuenda A, Banks L. (2006). Phosphorylation of the discs large tumour suppressor protein controls its membrane localisation and enhances its susceptibility to HPV E6-induced degradation. *Oncogene* **25**: 4276–4285.

Massimi P, Narayan N, Thomas M, Gammoh N, Strand S, Strand D *et al.* (2008). Regulation of the hDlg/hScrib/Hugl-1 tumour suppressor complex. *Exp Cell Res* **314**: 3306–3317.

Nagasaka K, Nakagawa S, Yano T, Takizawa S, Matsumoto Y, Tsuruga T *et al.* (2006). Human homolog of Drosophila tumor suppressor Scribble negatively regulates cell-cycle progression from

G1 to S phase by localizing at the basolateral membrane in epithelial cells. *Cancer Sci* **97**: 1217–1225.

Nakagawa S, Huibregtse JM. (2000). Human scribble (Vartul) is targeted for ubiquitin-mediated degradation by the high-risk papillomavirus E6 proteins and the E6AP ubiquitin-protein ligase. *Mol Cell Biol* **20**: 8244–8253.

Nakagawa S, Yano T, Nakagawa K, Takizawa S, Suzuki Y, Yasugi T *et al.* (2004). Analysis of the expression and localisation of a LAP protein, human scribble, in the normal and neoplastic epithelium of uterine cervix. *Br J Cancer* **90**: 194–199.

Navarro C, Nola S, Audebert S, Santoni MJ, Arsanto JP, Ginestier C *et al.* (2005). Junctional recruitment of mammalian Scribble relies on E-cadherin engagement. *Oncogene* **24**: 4330–4339.

Nola S, Sebbagh M, Marchetto S, Osmani N, Nourry C, Audebert S *et al.* (2008). Scrib regulates PAK activity during the cell migration process. *Hum Mol Genet* **17**: 3552–3565.

Pearson RB, Kemp BE. (1991). Protein kinase phosphorylation site sequences and consensus specificity motifs: tabulations. *Methods Enzymol* **200**: 62–81.

Pouyssegur J, Volmat V, Lenormand P. (2002). Fidelity and spatio-temporal control in MAP kinase (ERKs) signalling. *Biochem Pharmacol* **64**: 755–763.

Qin Y, Capaldo C, Gumbiner BM, Macara IG. (2005). The mammalian Scribble polarity protein regulates epithelial cell adhesion and migration through E-cadherin. *J Cell Biol* **171**: 1061–1071.

Sabio G, Arthur J, Kuma Y, Peggie M, Carr J, Murray-Tait V *et al.* (2005). p38gamma regulates the localisation of SAP97 in the cytoskeleton by modulating its interaction with GKAP. *EMBO J* **24**: 1134–1145.

Schaeffer HJ, Weber MJ. (1999). Mitogen-activated protein kinases: specific messages from ubiquitous messengers. *Mol Cell Biol* **19**: 2435–2444.

Tanoue T, Adachi M, Moriguchi T, Nishida E. (2000). A conserved docking motif in MAP kinases common to substrates, activators and regulators. *Nat Cell Biol* **2**: 110–116.

Thomas M, Massimi P, Navarro C, Borg JP, Banks L. (2005). The hScrib/Dlg apico-basal control complex is differentially targeted by HPV-16 and HPV-18 E6 proteins. *Oncogene* **24**: 6222–6230.

Torii S, Kusakabe M, Yamamoto T, Maekawa M, Nishida E. (2004). Sef is a spatial regulator for Ras/MAP kinase signaling. *Dev Cell* **7**: 33–44.

Torii S, Yamamoto T, Tsuchiya Y, Nishida E. (2006). ERK MAP kinase in G cell cycle progression and cancer. *Cancer Sci* **97**: 697–702.

Treisman R. (1996). Regulation of transcription by MAP kinase cascades. *Curr Opin Cell Biol* **8**: 205–215.

Yoon S, Seger R. (2006). The extracellular signal-regulated kinase: multiple substrates regulate diverse cellular functions. *Growth Factors* **24**: 21–44.

Zeitler J, Hsu CP, Dionne H, Bilder D. (2004). Domains controlling cell polarity and proliferation in the Drosophila tumor suppressor Scribble. *J Cell Biol* **167**: 1137–1146.

Zhan L, Rosenberg A, Bergami KC, Yu M, Xuan Z, Jaffe AB *et al.* (2008). Deregulation of scribble promotes mammary tumorigenesis and reveals a role for cell polarity in carcinoma. *Cell* **135**: 865–878.

Zhou T, Sun L, Humphreys J, Goldsmith EJ. (2006). Docking interactions induce exposure of activation loop in the MAP kinase ERK2. *Structure* **14**: 1011–1019.

British Journal of Cancer (2010) 102, 1061 – 1067

www.bjcancer.com

Identification of DBC1 as a transcriptional repressor for BRCA1

H Hiraike[1], O Wada-Hiraike*[,1], S Nakagawa[1], S Koyama[1], Y Miyamoto[1], K Sone[1], M Tanikawa[1], T Tsuruga[1], K Nagasaka[1], Y Matsumoto[1], K Oda[1], K Shoji[1], H Fukuhara[2], S Saji[3], K Nakagawa[4], S Kato[5,6], T Yano[1] and Y Taketani[1]

[1]Department of Obstetrics and Gynecology, Graduate School of Medicine, The University of Tokyo, Hongo 7-3-1 Bunkyo-ku, Tokyo 113-8655, Japan; [2]Department of Urology, Graduate School of Medicine, The University of Tokyo, Hongo 7-3-1 Bunkyo-ku, Tokyo 113-8655, Japan; [3]Tokyo Metropolitan Cancer and Infectious diseases Center Komagome Hospital, 3-18-22, Honkomagome, Bunkyo-ku, Tokyo 113 8677, Japan; [4]Department of Radiology, Graduate School of Medicine, The University of Tokyo, Hongo 7-3-1 Bunkyo-ku, Tokyo 113-8655, Japan; [5]SORST, Japan Science and Technology, Honcho 4-1-8, Kawaguchi, Saitama 332-0012, Japan; [6]Institute of Molecular and Cellular Biosciences, The University of Tokyo, Yayoi 1-1-1 Bunkyo-ku, Tokyo 113-0034, Japan

BACKGROUND: DBC1/KIAA1967 (deleted in breast cancer 1) is a putative tumour-suppressor gene cloned from a heterozygously deleted region in breast cancer specimens. Caspase-dependent processing of DBC1 promotes apoptosis, and depletion of endogenous DBC1 negatively regulates p53-dependent apoptosis through its specific inhibition of SIRT1. Hereditary breast and ovarian cancer susceptibility gene product BRCA1, by binding to the promoter region of SIRT1, is a positive regulator of SIRT1 expression.

METHODS: A physical interaction between DBC1 and BRCA1 was investigated both *in vivo* and *in vitro*. To determine the pathophysiological significance of DBC1, its role as a transcriptional factor was studied.

RESULTS: We found a physical interaction between the amino terminus of DBC1 and the carboxyl terminus of BRCA1, also known as the BRCT domain. Endogenous DBC1 and BRCA1 form a complex in the nucleus of intact cells, which is exported to the cytoplasm during ultraviolet-induced apoptosis. We also showed that the expression of DBC1 represses the transcriptional activation function of BRCT by a transient expression assay. The expression of DBC1 also inhibits the transactivation of the SIRT1 promoter mediated by full-length BRCA1.

CONCLUSION: These results revealed that DBC1 may modulate the cellular functions of BRCA1 and have important implications in the understanding of carcinogenesis in breast tissue.

British Journal of Cancer (2010) **102,** 1061 – 1067. doi:10.1038/sj.bjc.6605577 www.bjcancer.com
Published online 16 February 2010

Keywords: DBC1; BRCA1; interaction; repression

The gene encoding DBC1 (deleted in breast cancer 1) was identified during a representative differential analysis to search for candidate breast tumour-suppressor genes on a human chromosome 8p21 region that is frequently deleted in breast cancers (Hamaguchi *et al*, 2002). In this study, the expression of DBC2 (deleted in breast cancer 2) was substantially decreased in breast and lung cancer specimens. On the other hand, the expression of DBC1 was not substantially abrogated in cancers from any source. Molecular and cellular functions of DBC1 are currently extensively investigated to reveal the physiological role of DBC1 (Sundararajan *et al*, 2005; Kim *et al*, 2008; Zhao *et al*, 2008; Cha *et al*, 2009). Endogenous DBC1 is a nuclear protein and is thought to localise in the nucleus depending on its nuclear localisation signal (NLS) at the amino terminus. During tumor necrosis factor-α-induced apoptosis, DBC1 is translocated to the cytoplasm with loss of the NLS by caspase-dependent cleavage and this cleavage promotes apoptosis because of the death-promoting activity of its carboxyl-terminal coiled-coil domain (Sundararajan *et al*, 2005). Therefore, caspase-dependent cleavage of DBC1 may function as a positive feedback mechanism to promote apoptosis and this would explain how DBC1 functions as a tumour suppressor. A recent study demonstrated that DBC1 promotes p53-mediated apoptosis through specific inhibition of SIRT1, the mammalian homologue of yeast silent information regulator 2 (Sir2) (Kim *et al*, 2008; Zhao *et al*, 2008). However, functions of DBC1 in living cells still remain largely unknown and it should be determined whether DBC1 has a pivotal role in tumour suppression.

It is well known that the germ-line mutation of BRCA1 predisposes women to early-onset breast and ovarian cancer. BRCA1 is predominantly located in the nucleus and is involved in the basal transcriptional machinery (Scully *et al*, 1997; Anderson *et al*, 1998). BRCA1 regulates stress-inducible gene expressions such as p21 (Ouchi *et al*, 1998), p53 (Somasundaram *et al*, 1999), and GADD45 (Jin *et al*, 2000). The carboxyl-terminal BRCA1, referred to as the BRCT domain, has been shown to be involved in double-stranded DNA repair and homologous recombination (Callebaut and Mornon, 1997; Moynahan *et al*, 1999; Zhong *et al*, 1999). BRCT is indispensable for normal cellular growth

*Correspondence: Dr O Wada-Hiraike; E-mail: osamu.hiraike@gmail.com
Received 27 October 2009; revised 21 January 2010; accepted 25 January 2010; published online 16 February 2010

because the targeted deletion of the BRCT domain results in embryonic lethality (Hohenstein *et al*, 2001). The major function of BRCT is thought to be a gene regulator, mediating BRCA1 function as a tumour suppressor. This hypothesis is based on several lines of evidence, including that the autonomous transactivation function of BRCT was preserved in a recombinant protein consisting of the BRCT domain fused to a GAL4 DNA binding domain (Miyake *et al*, 2000). In addition, point mutations in the BRCT domain derived from patients with inherited breast cancer result in loss of transcriptional activity, and BRCA1 can also function as a negative regulator on some gene promoters (Chapman and Verma, 1996; Monteiro *et al*, 1996). This domain has already been shown to be an interaction surface with a number of transcription factors and co-regulators (Saka *et al*, 1997; Yarden and Brody, 1999; Wada *et al*, 2004; Oishi *et al*, 2006). A recent study revealed the interplay between SIRT1 and BRCA1 (Wang *et al*, 2008). BRCA1 was shown to stimulate the expression level of SIRT1 through binding to the specific promoter region of SIRT1, and this interplay prompted us to search for the cross talk between DBC1 and BRCA1.

To better understand the functional significance and the transcriptional regulation of BRCA1, we investigated the physical interaction between BRCA1 and DBC1. We found that DBC1 directly interacted with the BRCT domain. Our findings revealed that the amino terminus of DBC1 binds directly to the BRCT domain both *in vitro* and *in vivo*. We studied the effect of the transcriptional regulation of BRCA1 driven by DBC1. These findings establish a principal biological function of DBC1 in the modulation of BRCA1 function, and further identify DBC1 as a possible determinant and potential therapeutic target in breast cancer.

MATERIALS AND METHODS

Cell culture

Human cervical adenocarcinoma HeLa (CCl-2), human breast cancer MCF-7 (HTB-22), and human kidney 293T (CRL-11268) cell lines were purchased from the American Type Culture Collection (Manassas, VA, USA). These cells were maintained in Dulbecco's modified Eagle's medium supplemented with 10% foetal bovine serum.

Plasmid construction

BRCA1 expression vectors, BRCT vectors, and reporter constructs (17M8-AdMLP-luc) were described previously by Wada *et al*, 2004. DBC1 (Clone ID 5496068) and SIRT1 (Clone ID 4518906) expression vectors were purchased from Thermo Fisher Scientific Open Biosystems (Huntsville, AL, USA). Fragments of DBC1 were inserted into pcDNA-Myc vector derived from pcDNA3 (Invitrogen, Carlsbad, CA, USA).

Chemicals and antibodies

Rabbit polyclonal antibodies were anti-DBC1 (produced in our laboratory) and anti-acetyl-p53 (Upstate, Temecula, CA, USA, catalogue no. 06-758). Mouse monoclonal antibodies were anti-BRCA1 (Calbiochem, EMD Biosciences, Inc., LaJolla, CA, USA, catalogue no. OP93T), anti-Myc (Invitrogen, catalogue no. R95025), and anti-SIRT1 (Abnova, Taipei, Taiwan, catalogue no. H00023411-M01). Anti-BRCA1 (catalogue no. sc-642), anti-p21 (catalogue no. sc-397), anti-p53 (catalogue no. sc-126), and anti-actin (catalogue no. sc-47778) were purchased from Santa Cruz Biotechnology, Inc. (Santa Cruz, CA, USA). Alexa Fluor 488-conjugated donkey anti-mouse IgG (A-21202) and Alexa Fluor 555-conjugated goat anti-rabbit IgG (A-21428) were purchased from Invitrogen.

Immunoprecipitation and western blot

The formation of a DBC1–BRCA1 complex in HeLa and 293T cells was analysed by immunoprecipitation. The whole-cell extracts of HeLa cells were immunoprecipitated with anti-BRCA1 antibodies, and subsequently immunoblotted by anti-DBC1 antibodies. Reciprocal immunoprecipitation was also performed. Cells (293T) transfected with indicated plasmids were lysed and subjected to anti-FLAG M2 agarose (Sigma Aldrich, St Louis, MO, USA). Immunoprecipitated materials were blotted with anti-Myc antibodies to identify DBC1-containing complexes.

RNAi

The ablation of DBC1 and BRCA1 was performed by transfection of HeLa cells with small interfering RNA (siRNA) duplex oligos synthesised by Qiagen (Hilden, Germany). Control siRNA (AllStars Negative Control siRNA, Qiagen, 1027281), DBC1-specific siRNA (DBC1-RNAi: 5′-AAACGGAGCCUACUGAACA-3′, which covered mRNA regions of nucleotides 1379–1397 (amino acids 460–466) of DBC1, and KIAA1967-RNAi, SI00461853), and BRCA1-specific siRNA (#14 (SI02664361) and #15 (SI02664368)) were transfected using HyperFect reagent (Qiagen).

GST pull-down assay

Glutathione *S*-transferase (GST) fusion proteins or GST alone were expressed in *Escherichia coli* and immobilised on glutathione–sepharose 4B beads (GE Healthcare UK Ltd., Buckinghamshire, UK). GST proteins were incubated with [^{35}S] methionine-labelled proteins using a TNT-coupled transcription–translation system (Promega Co., Madison, WI, USA). Unbound proteins were removed and specifically bound proteins were eluted and analysed by SDS polyacrylamide gel electrophoresis.

Luciferase assay and mammalian two-hybrid assay

Transfection was performed with Effectene reagent (Qiagen) according to the manufacturer's recommendation. For luciferase assay, indicated expression vectors and GAL4 vectors were co-transfected with 17M8-AdMLP-luc or SIRT1-luc. For mammalian two-hybrid assay, GAL4 vectors and VP16 vectors were co-transfected. As an internal control to equalise transfection efficiency, phRL CMV-*Renilla* vector (Promega Co.) was also transfected in all experiments. Individual transfections, each consisting of triplicate wells, were repeated at least three times (Wada *et al*, 2004).

Fluorescence microscopy

Cells (MCF-7) were grown on 12 mm BD BioCoat glass coverslips (BD Biosciences, NJ, USA, 354085) in six-well plates before induction of apoptosis. The cells were treated or not treated with irradiation of ultraviolet (UV) light (0.24 J), fixed with phosphate-buffered saline (PBS) containing 4% paraformaldehyde, and permeabilised in PBS with 0.2% (v/v) Triton X-100. After blocking, the cells were incubated sequentially with anti-BRCA1 and anti-DBC1 antibodies. Secondary antibodies were Alexa Fluor 488-conjugated donkey anti-mouse IgG and Alexa Fluor 555-conjugated goat anti-rabbit IgG. The slides were briefly counter-stained and analysed under a confocal fluorescence microscope (Carl-Zeiss MicroImaging Inc., Oberkochen, Germany). Colocalisation was quantified using LSM7 series-ZEN200x software (Carl-Zeiss MicroImaging Inc.), and the ratio of colocalisation pixels *vs* total pixels in the target area was determined. The degree of colocalisation signal is expressed as mean ± standard deviation.

Immunohistochemistry

The procedure for immunohistochemical study has been described by Wada-Hiraike *et al*, 2006. The primary antibody used was anti-DBC1, and the ChemMate EnVision Detection system (DAKO, Carpinteria, CA, USA) was used to visualise the signal.

Chromatin immunoprecipitation assay

Soluble HeLa chromatin for PCR amplification was essentially prepared as described by Oishi *et al*, 2006. Subconfluent HeLa cells were crosslinked with 1.5% formaldehyde at room temperature for 15 min, and washed twice with ice-cold PBS. The cell pellet was then resuspended in 0.2 ml lysis buffer and sonicated by Bioruptor UCD-250 (Cosmo Bio, Co., Ltd., Tokyo, Japan). The sheared soluble chromatin was then subjected to immunoprecipitation with specific antibodies and protein G-sepharose with salmon sperm DNA (Upstate). After an extensive wash, the beads were eluted. The eluate was incubated for 6 h at 65°C to reverse the formaldehyde crosslink. The extracted DNA was purified using the QIAquick PCR purification kit (Qiagen). PCR was performed using specific primers (Wang *et al*, 2008).

RESULTS

DBC1 and BRCA1 interact *in vivo* and *in vitro*

To determine the interaction between endogenous DBC1 and BRCA1 in cultured human cells, cell extracts from HeLa cells were immunoprecipitated with anti-BRCA1 antibodies or with preimmune IgG. The immunoblotting analysis using anti-DBC1 antibodies revealed the existence of DBC1 in cell lysate immunoprecipitates (Figure 1A), which indicates that DBC1 physically associates with BRCA1 in living cells. Reciprocal immunoprecipitation analysis confirmed this association (Figure 1A). In addition, Flag-tagged BRCA1 and Myc-tagged DBC1 were each transfected in 293T cells and extracts of transfected cells were immunoprecipitated with anti-FLAG M2 agarose beads. Western blotting analysis with anti-Myc antibodies revealed the existence of Myc-tagged DBC1 in the protein extract of immunoprecipitates (Figure 1B),

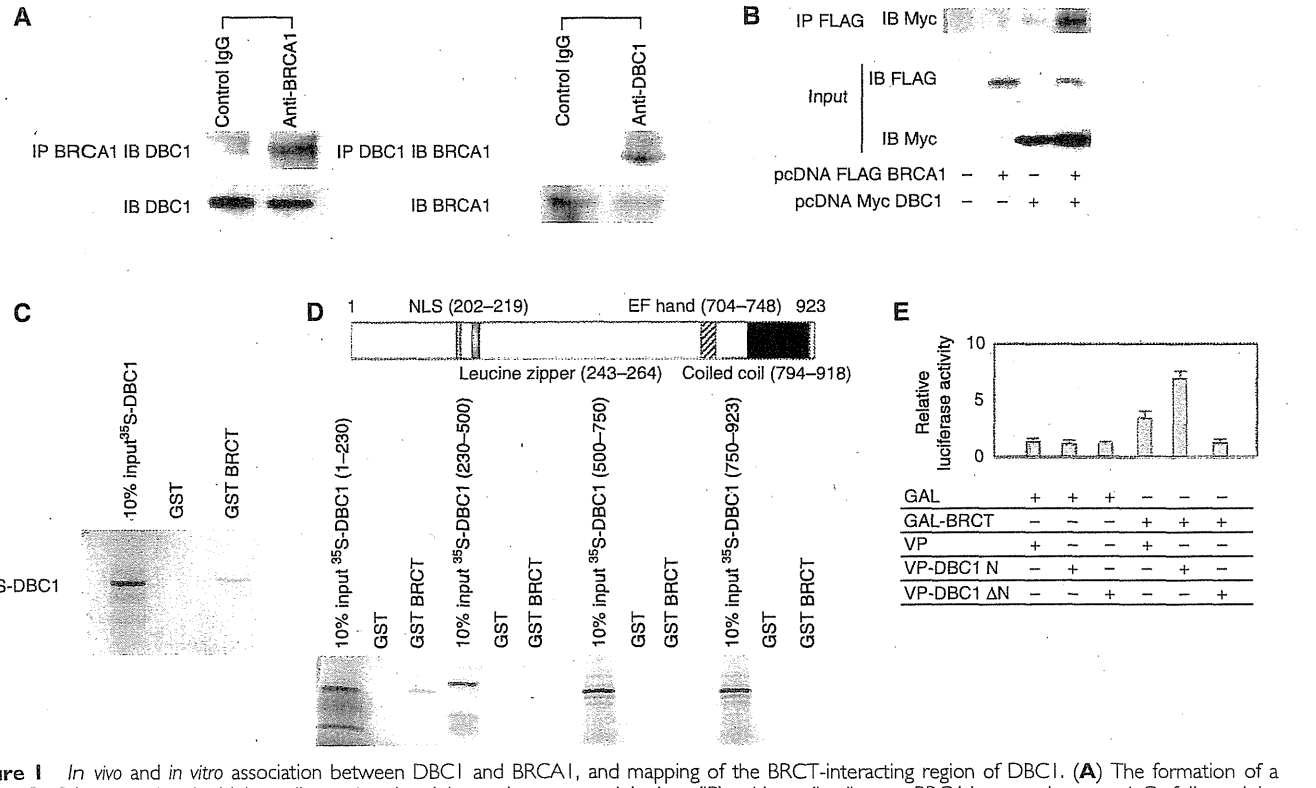

Figure 1 *In vivo* and *in vitro* association between DBC1 and BRCA1, and mapping of the BRCT-interacting region of DBC1. (**A**) The formation of a DBC1–BRCA1 complex in HeLa cells was analysed by co-immunoprecipitation (IP) with antibodies to BRCA1 or preimmune IgG, followed by immunoblotting (IB) using anti-DBC1 antibodies. The immunoprecipitates were subjected to 30 μl of protein G sepharose 4 Fast Flow and bound proteins were detected by western blotting. Reciprocal co-immunoprecipitation with antibodies to DBC1 and subsequent IB confirmed the complex formation of DBC1 and BRCA1. (**B**) The formation of a DBC1–BRCA1 complex in 293T cells was analysed by IP with anti-Flag M2 agarose beads, followed by IB using anti-Myc antibodies. Bound proteins were detected by western blotting. (**C**) Mapping of the BRCT-interacting region of DBC1 using glutathione *S*-transferase (GST)–BRCT and DBC1. Bacterially expressed GST fusion proteins immobilised on beads were used in *in vitro* pull-down assays. Full-length DBC1 was *in vitro* translated in the presence of [^{35}S] methionine using a TNT-coupled *in vitro* translation system. Labelled DBC1 was then incubated with GST–BRCT. The mixtures were washed and subjected to SDS polyacrylamide gel electrophoresis (PAGE) and analysed. Polyacrylamide gels were stained briefly with Coomassie Brilliant Blue to verify the loading amounts of fusion proteins. (**D**) A schematic diagram of the structure of DBC1 is shown. Fragments of DBC1 ((amino acids 1–230), (230–500), (500–750), and (750–923)) were *in vitro* translated using a TNT-coupled *in vitro* translation system. Labelled DBC1 was incubated with GST–BRCT. The mixtures were extensively washed and subjected to SDS–PAGE and then analysed by autoradiography. (**E**) Mammalian two-hybrid interaction analysis. Cells (293T) were transfected with the indicated combinations of mammalian expression vectors encoding GAL4, GAL4–BRCT, the herpes simplex virus VP16 transactivation domain (VP16), and VP16-DBC1 chimera. At 24 h after transfection, cells were harvested, and transfected whole-cell lysates were assayed for luciferase activity produced from a co-transfected GAL4 DNA binding site-driven reporter template (17M8-AdMLP-luc). GAL–BRCT shows additive transactivation when co-transfected with VP-DBC1 N, suggesting the interaction between BRCT and DBC1 (1–230) *in vivo*.